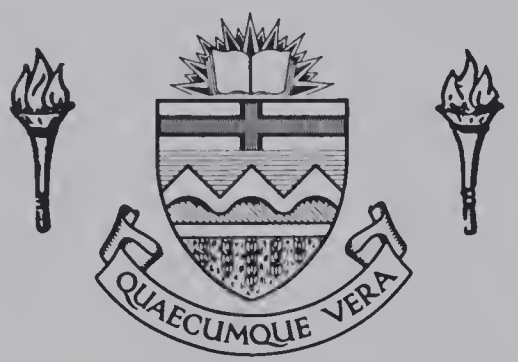

THE UNIVERSITY OF ALBERTA

RELEASE FORM

NAME OF AUTHOR Richard Warren Bailey

TITLE OF THESIS Flexural and Shear Behaviour of Large Diameter Steel Tubes

DEGREE FOR WHICH THESIS WAS PRESENTED Master of Science

YEAR THIS DEGREE GRANTED Spring, 1984

THE UNIVERSITY OF ALBERTA

Flexural and Shear Behaviour of Large Diameter Steel Tubes

by

Richard Warren Bailey

A THESIS

SUBMITTED TO THE FACULTY OF GRADUATE STUDIES AND RESEARCH

IN PARTIAL FULFILMENT OF THE REQUIREMENTS FOR THE DEGREE

OF Master of Science

Department of Civil Engineering

EDMONTON, ALBERTA

Spring, 1984

THE UNIVERSITY OF ALBERTA

FACULTY OF GRADUATE STUDIES AND RESEARCH

The undersigned certify that they have read, and recommend to the Faculty of Graduate Studies and Research, for acceptance, a thesis entitled Flexural and Shear Behaviour of Large Diameter Steel Tubes submitted by Richard Warren Bailey in partial fulfilment of the requirements for the degree of Master of Science.

Abstract

In this study, the flexural and shear behaviour of large diameter fabricated steel cylinders was experimentally investigated and the results compared with those obtained from existing design equations. The first part of the experimental program consisted of testing an unstiffened cylinder (R/t = 174) in pure flexure. The objective was to add to the scarce data base on cylinders in flexure. The results were compared to those obtained using the semi-empirical design equation of Stephens, et al. for axially loaded cylinders. The objective of the comparison was to evaluate the equation's applicability to design in flexure.

In the second part of the program, a longitudinally stiffened cylinder (R/t = 128) was tested in flexure. The theoretical strength of the cylinder was calculated using existing design methods for longitudinally stiffened cylinders loaded in axial compression. The objective was to investigate the applicability of these theories to flexural behaviour.

In the last part of the test program, two cylinders (R/t = 251, 75) were loaded primarily in transverse shear. The results were compared to classical theory of elastic buckling in pure and transverse shear. The objective was to identify the behaviour parameters in shear and the tension field contribution to post-buckling strength.

Although the test evidence is still limited, the Stephens, et al. semi-empirical design equation does provide

a good prediction of the strength of unstiffened cylinders loaded in flexure. Published methods for predicting first yield and buckling of longitudinally stiffened cylinders loaded in axial compression give conservative results for a flexurally loaded stiffened specimen, but the experimental data are limited. The strength of a cylinder loaded primarily in transverse shear is dependent largely on the R/t ratio of the specimen, the presence of residual stresses, and the support conditions.

Further testing is needed in all areas. Unstiffened cylinders with high R/t ratios should be further tested in pure flexure, as the data base is limited. A series of longitudinally stiffened cylinders of varying R/t ratios with different stiffener sizes and spacings should be tested in flexure with the objective of establishing the differences that exist between the strength of cylinders loaded in axial compression and those loaded in bending. The problem of shear loading of fabricated steel cylinders is still largely unexplored. Further physical testing in the R/t range of interest is required and a theoretical basis for predicting the test results has to be established.

Acknowledgements

I wish to thank Dr. G. L. Kulak and Dr. A. E. Elwi for their supervision and guidance throughout the course of this work.

The advice and assistance of L. Burden and R. Helfrich during the experimental phase of the work and the invaluable help of Thomas Casey in computer-related areas are greatly appreciated.

Table of Contents

List of Tables

List of Figures

List Of Symbols

a_o = normalized imperfection amplitude (ω_o/t)

b = panel width of longitudinally stiffened shell

D = cylinder diameter

E = modulus of elasticity

L = cylinder length

m = Koiter buckling parameter

R = cylinder radius

t = cylinder wall thickness or plate thickness

V_t = vertical force component of tension field

V_u = ultimate shear strength

V_y = shear yield strength of cylinder

W = developed width of tension field

α = arc covered by tension field

γ_s = nondimensional buckling parameter

ζ = angle of inclination of tension field

θ = Koiter's shell buckling parameter

ν = Poisson's ratio

ϕ_{cr} = angle between stiffeners at point when cylinder behaviour becomes "narrow"

ϕ_o = angle between stiffeners on a longitudinally stiffened shell

σ_{br} = Brazier buckling stress of a thin-walled cylinder

σ_{cl} = classical elastic buckling stress of a thin-walled cylinder

σ_{cr} = critical buckling stress of a stiffened cylinder

σ_u = ultimate buckling stress of a thin-walled cylinder

σ_y = yield stress

σ_{ys} = static yield stress

ω_o = imperfection amplitude

1. Introduction

1.1 Large Diameter Fabricated Steel Members

Large diameter circular steel shells, both stiffened and unstiffened, are often used in civil engineering structures. Storage tanks, columns, conveyor galleries, and offshore structures are some examples of structures incorporating these shells.

For the past several years, a research program into the behaviour of large-diameter fabricated steel cylinders has been carried out at the University of Alberta. Radius-to-thickness ratios (R/t) in the order of 150 to 225 have been examined, and both experimental and analytical studies have been included (1,2,3). This report is a continuation of that work.

Three main topics are covered. First, the behaviour of unstiffened, large diameter cylinders loaded in pure flexure is investigated. Second, the behaviour of longitudinally stiffened, large diameter cylinders loaded in pure flexure is examined, and third, the behaviour of unstiffened cylinders loaded primarily in shear is investigated.

1.2 Statement of Problem

The data base for the flexural behaviour of unstiffened fabricated steel cylinders is very small at the present time. A semi-empirical design equation has been developed (1), but needs to be tested further. An analytical method

for predicting the strength of axially loaded cylinders is available (2,3) and the work is being extended to include members loaded in flexure. The purpose of the test reported here was to add to the data base of experimental work, using in particular a more slender cylinder than had been previously tested.

Although much work has been done on longitudinally stiffened cylinders, a large fraction of this work has been on aerospace quality specimens. Of the remainder, the major proportion has been on axially compressed specimens. Very few tests in pure flexure on fabricated steel specimens have been performed.

Little has been found in the literature on experimental work on cylinders loaded in transverse shear. Theories exist for calculating shear strength for curved panels and cylinders in pure shear, although these theories do not consider the inevitable additional stresses due to bending, and their ability to include the post-buckling contribution to strength is unknown.

1.3 Objectives

The objectives of this study were:

1. To test an unstiffened large diameter fabricated steel cylinder loaded in flexure only and to compare the test results with recently proposed design equations (1).
2. To test a longitudinally stiffened large diameter

fabricated steel cylinder loaded in flexure only, and to examine the applicability of existing design methods for axially loaded longitudinally stiffened cylinders to those loaded in flexure, and to compare test results with these methods.

3. To test unstiffened cylinders loaded primarily in shear, and to investigate the possibility of developing an ultimate strength equation for cylinders loaded in shear.
4. To make recommendations for further testing.

2. Review of Cylinder Behaviour

2.1 Introduction

In this chapter past work done on cylinders is reviewed. The problem of unstiffened cylinders loaded in axial compression and flexure is reviewed, followed by a review of longitudinally stiffened cylinders under axial compression and flexure. This is followed by a review of the behaviour of unstiffened cylinders loaded primarily in shear.

2.2 Buckling of Unstiffened Cylinders

2.2.1 Overview

In 1981, Stephens, et al. (1) reported on a literature survey on theories available for predicting the strength of unstiffened cylinders in axial compression and in flexure. Sections 2.2.1, 2.2.2 and 2.2.3 herein are largely a summary of this work.

When a structure fails, either through physical collapse or inability to carry the applied load, at loads less than those required to produce material failure, it is said to have buckled. Thin-walled cylinders of the type looked at in this study are susceptible to this form of failure.

The type of buckling which a cylinder undergoes is dependent on the member geometry and loading conditions. Overall buckling occurs when the entire structure becomes

unstable, leading to collapse. If failure due to instability of only a portion of the cylinder wall occurs before the entire member becomes unstable, local buckling is said to have occurred.

If a geometrically perfect cylinder is assumed, then the loading behaviour up to and including buckling can be described using a small-displacement theory. However, a real structure will contain initial geometric imperfections, with the result that the theories based on the assumption of an initially perfect cylinder are no longer applicable. Thin-walled cylinders in particular are quite sensitive to initial imperfections, and they can be expected to buckle at loads less than those theoretically predicted.

Buckling may be further described as either elastic or inelastic. Elastic buckling describes that case in which the cross-sectional properties remain elastic, i.e., no yielding has occurred. Thus, the yield strength of the material does not enter into consideration (except to identify the limit of the range). When buckling occurs after some part or parts of the cross-section have yielded, inelastic buckling is said to have occurred, and the description of behaviour will include the yield point of the material.

The early theories developed to describe thin-walled cylinder stability consider a geometrically perfect member, elastic material behaviour, and linear relationships between displacements, strains, and curvature. These "classical" stability theories are based on the assumption of small

displacements, and preclude initial geometric imperfections.

2.2.2 Unstiffened Cylinders Under Axial Compression

The classical theoretical analysis of local buckling of unstiffened cylinders under axial compression was performed mainly by Timoshenko (4), Southwell (5), Flügge (6), and Donnell (7). As a result of this work, it was shown that elastic buckling depends on a number of parameters. These include dimensional parameters such as length (L), radius (R), and thickness (t), and material properties such as the modulus of elasticity (E) and Poisson's ratio (ν). These theories describe three types of behaviour for axially compressed cylinders, differentiated by the L/R ratios as follows:

1. Short cylinders ($L/R < 1.72(t/R)^{1/2}$). These behave as stub columns or axially compressed flat plates.
2. Long cylinders ($L/R > 2.85(R/t)^{1/2}$). These behave as long columns, and fail due to overall elastic (Euler) buckling.
3. Intermediate cylinders. These fall between the above limits, and will buckle in either an asymmetric or an axisymmetric mode.

Buckling of cylinders in the intermediate region is independent of length and mode of buckling (4,6). A cylinder with simply supported edges has a classical (elastic) buckling strength (4) of

$$\sigma_{cr} = \frac{1}{[3(1-\nu^2)]^{1/2}} \frac{Et}{R} \qquad (2.1)$$

As a cylinder nears the transition from medium to long cylinders, interaction between the overall column buckling and local buckling in the asymmetric mode may lead to a reduction of the critical buckling stress indicated by Eq. 2.1 (8).

Experiments have shown that the actual buckling loads of thin-walled cylinders are quite different from those predicted by classical theory. For axially compressed cylinders, test results often average 1/2 to 1/3 of the classical load, and show large scatter.

In 1941, von Kármán & Tsien (9) developed an approximate numerical analysis based on Donnell's elastic nonlinear finite displacement theory (7). This analysis indicated that equilibrium states involving large displacements can be maintained by smaller loads than the critical load obtained from classical small-displacement theory.

In 1945, Koiter (10) incorporated finite initial imperfections into his general nonlinear stablility theory. This theory predicts the maximum load that can be maintained before buckling occurs, and relates this load to the size of the imperfection causing the buckling. In general, the larger the initial imperfection, the smaller the buckling load.

The inclusion of initial imperfections provides a theoretical explanation for buckling at loads less than the

classical value, and as well helps to account for the large amount of scatter observed in tests. Because the amplitudes of initial imperfections are statistically random, scatter in the results is to be expected.

Koiter's derivation originally assumed imperfections were axisymmetric in shape. Tests performed on cylinders with axisymmetric imperfections milled into the walls showed good correlation between theory and test. Further investigation by Koiter (11) showed that interaction between axisymmetric and asymmetric imperfections resulted in a greater reduction in strength than axisymmetric imperfections acting alone.

Recent analyses by Arbocz (12) and Babcock (13) involving numerical techniques applied to single and multiple mode interactions and random imperfection amplitudes have been able to predict the elastic buckling loads of test specimens with a fair degree of accuracy.

Stephens, et al. (1) developed a semi-empirical design formula, based on their tests and a review of tests by others, for structural quality fabricated steel cylindrical shells in axial compression. This formula, which does have a theoretical foundation, was found to accurately predict specimen behaviour. It is fairly simple, and is suitable for design work. It is based on a buckling parameter γ_s, where

$$\gamma_s = (E/\sigma_{ys})^{1/2}(t/R)^{3/2} \qquad (2.2)$$

Using this parameter, a series of best fit curves to

available test data was established, yielding the following equations:

$$\frac{\sigma_u}{\sigma_{ys}} = 119.3\gamma_s \qquad \gamma_s \leq 0.0036 \qquad (2.3)$$

$$\frac{\sigma_u}{\sigma_{ys}} = 1.625 + 0.489 \log\gamma_s \qquad 0.0036 < \gamma_s < 0.0527 \qquad (2.4)$$

$$\frac{\sigma_u}{\sigma_{ys}} = 1.0 \qquad \gamma_s \geq 0.0527 \qquad (2.5)$$

These equations give the buckling stress as a fraction of the static yield stress.

Recently, the finite element program NISA 80 has been used by Pinkney, et al. (2,3) to predict the buckling of axially loaded cylindrical shells. This analysis incorporates measured initial imperfections and material nonlinearities, enabling the equilibrium path to be traced up to and beyond the limit point. An elastic - perfectly plastic material model was used, with the imperfection amplitudes measured from specimens tested by Stephens, et al. (1). The predictions obtained using this analysis compare closely with the experimental results.

2.2.3 Unstiffened Cylinders Under Flexure

The first attempt at a solution for local buckling of cylinders in flexure was performed by Flügge in 1932 (6). Flügge investigated the buckling behaviour under combined axial compression and bending for a particular radius to thickness ratio, and a particular buckle wavelength to radius ratio. From this analysis, he concluded that the minimum critical stress for bending was 30% greater than

that for axial compression alone. Timoshenko (4) cited this result without a qualifying statement as to the assumed buckle wavelength, and it has since been adopted as a general rule.

In 1961, Seide and Weingarten (14) performed a numerical analysis using small displacement theory. Their results indicated that Flügge's assumed critical wavelength was incorrect, and that the flexural buckling stress is approximately equal to the compressive buckling stress.

In 1927, Brazier (15) investigated a limit point buckling mode found in flexurally loaded tubes, which has since come to be called "the Brazier effect". When a long cylindrical tube is subjected to a bending moment, it assumes a curvature. Because of this bending induced curvature, the longitudinal tension and compression stresses will be accompanied by transverse stresses which have components directed towards the mid-plane of the tube. The effect of these components is to squeeze the tube into an oval shape, thereby reducing its resistance to bending. By applying a small-displacement theory to a tube of infinite length, Brazier determined the limit point moment. If the longitudinal bending stress is based on the geometry of the undeformed cross-section, this moment corresponds to a critical axial stress of

$$\sigma_{br} = \frac{2}{9}\left[\frac{2}{(1-\nu^2)}\right]^{1/2}\frac{Et}{R} \qquad (2.6)$$

which is approximately one-half the classical compressive

buckling stress.

This tendency towards ovaling leads to the possibility of buckling occurring at a reduced moment after considerable ovaling had taken place. The flattening of the cross-section would result in larger stresses for a given moment, and the critical buckling stress would be lower because of the increase in the local radius of curvature at the point of maximum stress.

This type of buckling can be prevented by the insertion of bulkheads or circumferential stiffeners, which will prevent any significant ovaling from taking place. Cylinders thus restrained can be analysed considering only the buckling behaviour of the undeformed circular cross-section.

Although small-displacement theory indicates the buckling stress in flexure is approximately the same as that for axial compression, some experimental results have shown a higher buckling stress for flexurally loaded members. At present, no large-displacement buckling analysis exists to show whether the increase in buckling stress for cylinders in bending is an inherent characteristic.

Some conceptual reasons have been put forward to explain this higher buckling stress. It has been observed that the buckle pattern for cylinders in bending is similar to that obtained from axial compression. This leads to the assumption that the buckling behaviour is similar for both cases. Since the flexural stress distribution varies circumferentially, there will be a preferred region of buckling.

The probability of imperfections occurring in this region is less than that for the entire circumference, leading to a higher buckling stress on the average. However, there would be cases in which the stresses in bending would approach those in axial compression. Further, an increase in flexural buckling strength relative to the compressive strength is indicated, based on a review of test results for aerospace quality specimens by Seide, et al. (16) and Weingarten, et al. (17). Another explanation put forth is that the the strain gradient resulting from the circumferentially varying bending stress may be responsible for the increase.

In 1981 Stephens, et al. (1) performed a series of tests on steel cylinders loaded in compression and in flexure. Some small scale cylinders (191 mm radius, 0.89 mm wall thickness) were tested in axial compression, but the main thrust of the experimental work was the testing of two matched pairs of large cylinders, with one of each pair being tested in axial compression, and the other in pure flexure. One pair had a radius of 765 mm, with a wall thickness of 5.13 mm (R/t = 149), and the other pair had a radius of 762 mm with a wall thickness of 3.43 mm (R/t = 222). It was found that the proportional limits for the compressive test and the bending test were very close. The first pair buckled at 60% of yield in compression and 61% in flexure, with the second pair buckling at 59% of yield in compression and 62% in flexure.

Based on these observed experimental results and the fact that the experimental data base for structural members in flexure is small, Stephens, et al. recommended that the buckling stress for axial compression also be used for bending of structural steel cylinders. The semi-empirical formula derived by them provides an easy design method for determining the critical stress.

2.3 Buckling of Longitudinally Stiffened Cylinders

The buckling strength of circular shells can be substantially increased by the addition of ring and/or longitudinal (stringer) stiffeners. As the increase in weight is not great in comparison to the strength increase, this may provide a good method of increasing load capacity if design conditions permit.

Failure of stiffened shells can occur by either local buckling of the cylinder wall between stiffeners (panel instability), or by buckling of the cylinder as a whole (general instability). Panel instability will occur in wide-panelled shells, while general instability occurs when the stiffener spacing is such that a shell is narrow-panelled. This will be discussed in more detail later.

The problem of flexural buckling of stiffened shells can be related to that of stiffened shells under axial compression. Therefore, a review of work done in that area follows.

2.3.1 Longitudinally Stiffened Shells Under Axial Compression

Since the 1940's, there has been extensive testing of longitudinally stiffened shells under axial compression, due mainly to their extensive use in aeronautical and aerospace structures. However, because the shells used in these industries are usually made of very thin, high quality aluminum, as opposed to the thicker structural steel used in civil engineering structures, the results are not completely relevant. The differences can be summarized as follows: (18)

1. The thin aluminum aerospace shells usually fail by elastic buckling, while the structural steel shells are usually proportioned so that yielding occurs before collapse.
2. Aluminum and steel have different stress-strain characteristics.
3. The rolling and welding of the steel shells leads to geometric imperfections and residual stress levels different from those in the integrally machined aluminum shells.
4. The stiffeners in cylinders used in offshore work are usually spaced further apart and provide less rotational restraint to the plate than those used in aerospace structures.

As mentioned earlier, a wide-panelled shell will buckle in the same manner as a similar unstiffened shell, while a narrow-panelled shell will have a higher critical stress. In

1956, Koiter (10) studied buckling and post-buckling behaviour of cylindrical panels with stringers that exerted no rotational restraint on the panel. His analysis showed that narrow panel behaviour will occur when the angle between equally spaced stiffeners, ϕ_o, is less than π/m, where

$$m = \tfrac{1}{2}[12(1-\nu^2)]^{1/4} (R/t)^{1/2} \qquad (2.7)$$

The increase in stiffness of this panel, due to the narrow panel behaviour is

$$\frac{\sigma_{cr} \text{ (narrow)}}{\sigma_{cr} \text{ (complete)}} = (1/\theta^2)(1 + \theta^4) \qquad (2.8)$$

using

$$\theta = \frac{m\phi_o}{\pi} = \frac{[12(1-\nu^2)]^{1/4}}{2\pi} \, b(Rt)^{-1/2} \qquad (2.9)$$

where

b = panel width between stiffeners

In 1963, Baruch and Singer (19) developed a method of analysis for stiffened shells under hydrostatic pressure, using a "distributed stiffness" method. This method models the stiffened shell as an unstiffened shell with orthotropic material properties, taking into account the geometry of the stiffened shell. Singer, et al. (20) applied this method to the problem of stiffened shells under axial compression, developing a method for finding the critical axial load of shells with both simply supported and clamped ends.

A simplified method of determining the collapse load of an axially compressed longitudinally stiffened shell was

proposed by Walker and Sridharan (21) in 1980. This analysis uses an equivalent column model. The representative column is a stiffener taken together with half panels to either side. To account for continuity, the column is treated as a body resting on an elastic medium. To find the stiffness of this medium, the critical stress of the model is equated to the neutral equilibrium stress of an equivalent plate structure. This critical stress is found numerically by using an energy method, and interpolating to find the number of circumferential waves into which the shell will buckle. The column model can take into account the effects of initial imperfections, residual stresses, and local buckling, with the analysis proceeding in a manner comparable to that for stiffened flat plates. The failure criterion used for this model is the load at which first yield, either in the stiffener or the plate, occurs.

Walker and Sridharan related their theoretical work to an experimental program they performed in 1979 (22). The specimens tested were 1/20 scale models of offshore components, with R/t ranging from 200 to 360, and the number of stiffeners ranging from 20 to 40. These stiffener spacings gave both narrow and broad panelled cylinders. It was found that the theoretical model predicted the experimental collapse stress fairly closely, with the test to predicted ratio ranging from 0.87 to 1.01.

At present, research into structural quality stiffened shells is mainly related to offshore structures. In Great

Britain, the Department of Energy is sponsoring a coordinated research program, with the Science and Engineering Research Council the primary sponsor of theoretical studies (23). The Norwegian classification society, Det norske Veritas (DnV), is involved in structural steel offshore components. DnV design rules for offshore structures (24) cover longitudinally stiffened cylindrical shells, and, under their sponsorship, investigations are continuing into the development of analytical models accounting for local buckling of the stringers on broad-panelled cylinders, and on studies of multispan interaction effects (25).

In Japan, research into offshore structures is also active (26). Research into longitudially stiffened cylindrical shells seems to be mainly theoretical, however. In North America, the Chicago Bridge and Iron Company (27) is performing a series of tests on ring and stringer stiffened cylinders under various loading conditions.

2.3.2 Longitudinally Stiffened Shells Under Flexure

As the main thrust of research on longitudinally stiffened shells is in offshore structures, and since these elements are usually under axial compression and/or hydrostatic pressure, there has been little work relating to the problem of longitudinally stiffened shells under flexure.

Fujita, et al. (28) have done theoretical work on cylindrical shells with longitudinal stiffeners and transverse rings under axial compression and pure bending. The elastic

behaviour equations were developed by applying Galerkin's method to Donnell's shell equations, and adding the stiffness terms to account for the stiffeners and rings. After panel buckling, the stiffener buckling load was determined by a framework model, with the effective width of the stiffeners being determined iteratively. It was found that the buckling load of the panel can be closely predicted by the theory, but that the buckling load of the frame structure stiffened by the longitudinal stiffeners and transverse rings is over-estimated, with the test values being about 80% of the theoretical prediction.

2.4 Unstiffened Cylinders Under Shear Loading

The presence of shear stresses in a cylinder can result from either torsional or transverse loads. The current study is concerned only with the shear stresses that result from transverse loading, i.e., those shear stresses which result from the flexural action of the member.

Little experimental or theoretical work on cylinders loaded in transverse shear has been found in the literature. Schilling (8) refers to tests done by E. G. Lundquist on aerospace quality Duralumin cylinders. In these tests, transverse shear stresses causing local buckling averaged 60% higher than shear stresses for torsional buckling. Schilling suggests that for elastic buckling, a conservative value of 1.25 times the critical torsional shear buckling stress be used for cylinders loaded in transverse shear.

Batdorf, et al. (29,30) developed theoretical solutions relating to the critical shear stress of curved rectangular plates. Their results are based on small deflection theory for panels with simply supported and clamped edges, and are given as a series of curves for varying panel dimensions. These curves are found to be in good agreement with test results.

Wilson and Olsen (31) tested a number of steel cylinders under a variety of loading conditions, including axial loads, transverse loads, and combined axial and transverse loads. Tests of cylinders loaded as simply supported beams included machined specimens having an outside diameter of 102 mm, with a wall thickness of 1.6 mm, and loaded at midspan. The effective lengths (the distance between the load point and the end support) varied from 64 to 165 mm. Fabricated specimens were also tested. They had outside diameters ranging from 711 to 762 mm, with a wall thickness of 6 mm. These were loaded by a two point system, with effective lengths from 305 to 914 mm.

One type of structural member that is often loaded primarily in shear is the plate girder. The strength of plate girders loaded primarily in shear is usually calculated using the tension field theory proposed by Basler in 1961 (32). Although many other approaches have been suggested, with the most important summarized in Ref. 33, the Basler theory is relatively uncomplicated and gives reasonable results. It is used as the basis for most design

specifications in North America.

This theory recognizes the fact that after a plate loaded in shear buckles, the load-carrying mechanism changes, with significant post-buckling strength. The theory suggests that the shear strength consists of both buckling and post-buckling contributions. Prior to buckling, shear capacity is due to beam action, while after buckling shear resistance results from the formation of a tensile field in the web. This field will form diagonally between vertical stiffeners which act as reaction points for the field. The analogous part of the cylinder would be a ring stiffener or support. Although no such theory has been found in the literature, it may be possible to adapt the tension field theory to cylinders under transverse shear.

3. Experimental Program

3.1 Introduction

The purpose of the experimental program is threefold. First, it is desirable to increase the data base for the strength of unstiffened thin-walled fabricated steel cylinders in pure flexure, both because there have been very few tests of this type performed, and to further evaluate the semi-empirical design method previously developed (1). Second, since few large-scale flexural tests of longitudinally stiffened thin-walled cylinders have been reported, it is necessary to investigate this type of behaviour. Third, for the same reasons, the behaviour of unstiffened thin-walled cylinders loaded primarily in shear warrants investigation.

3.2 Initial Imperfections

Both theoretical and experimental research indicates that initial imperfections can influence the flexural buckling strength of fabricated steel cylinders. Therefore, it is desirable that the amplitude and location of such imperfections be measured.

At the time of the first shear test, the role of imperfections was unknown. Thus, extensive imperfection measurements were taken for this case. Based on the results of the first test, it was concluded that imperfections do not play a significant role in the shear behaviour, and it was

therefore decided that only qualitive measurements were needed for the second test.

3.2.1 Apparatus and Measuring Procedure

3.2.1.1 Unstiffened Flexural Specimen

The apparatus used to measure imperfections consisted of a series of dial gauges mounted at intervals along an aluminum channel. At right angles to the channel, an arm was fastened which pivots about a central point. The device thus measures specimen radii with respect to some assumed longitudinal axis.

As will be more fully described later, the flexural specimen consisted of a thin central region, with thicker end portions. This arrangement was selected in order to force the cylinder to buckle in the central region. Because of this configuration, imperfection measurements were concentrated mainly in the central region, with a dial gauge spacing of 115 mm, and a wider spacing, 305 mm, in the end zones. The spacing was further decreased in the vicinity of the circumferential welds. The circumferential arc distance used for the readings was 173 mm (corresponding to an arc of 11.25°). This produced 32 radial measurements at each of 21 different locations along the length of the member, for a total of 672 measurements of initial imperfection.

3.2.1.2 Stiffened Flexural Specimen

The measuring apparatus used was similar to that used for the unstiffened specimen, except that instead of a series of gauges, one gauge was mounted on a slide that could be moved up and down the channel to the locations selected for readings.

A spacing of 100 mm in the longitudinal direction was generally used to measure imperfections in the cylinder. In the vicinity of the circumferential welds, the spacing was decreased to 50 mm. The circumferential arc length was 255 mm (corresponding to an arc of 22.5°). This gave 16 radial measurements at each of 21 locations along the length of the member, for a total of 336 measurements of initial imperfection.

To measure imperfections in the stiffeners, a straight-edge was laid along the stiffener, and "feeler gauges" (thin metal strips of known thickness), were used to determine the out-of-straightness.

3.2.1.3 Shear Specimens

The shear specimens consisted of a cylinder with fixed ends, loaded in the centre, with two thinner portions in the regions of minimum moment. The thinner sections were intended to fail in shear, and the measurements of imperfections were therefore concentrated in these areas.

Imperfection measurements of the first shear specimen were taken differently from those of the large flexural specimens. Because the specimen was relatively small, the

measurements of imperfections were made externally. The specimen was mounted between two pivots, so that it could rotate about a longitudinal axis. A dial gauge was mounted on a bracket which could slide along a fixed channel, with the dial gauge contacting the specimen. Thus, with the dial gauge moved into position, the specimen was rotated to take measurements, and the dial gauge was then moved longitudinally and the process was repeated.

Readings were taken at 25 mm intervals along the length of the shear spans, decreasing in the vicinity of the seam welds. The arc distance of 37 mm, corresponding to an arc of 11.25°, gave 32 radial measurements. These were taken at 41 locations, for a total of 1312 measurements of initial imperfection.

It was observed during the testing of the first shear specimen that imperfections did not appear to play a significant role in strength reduction. A large deformation was incurred during the welding process, and subsequently pulled out. This left large initial imperfections in that area, far larger than any measured elsewhere, but the span with this deformation did not appear to behave significantly differently than the intact span. Therefore, quantitative imperfection measurements were not taken on the second specimen. A straightedge was placed on the cylinder, and depressions or bulges in the shell were noted.

3.3 Unstiffened Flexural Specimen

3.3.1 Specimen Description

The specimen was fabricated from steel meeting the requirements of CSA Specification G40.21M 700Q (34). The central portion was 1219 mm in length, and was made of 5 mm thick plate. The two end sections, each 760 mm in length, were made from 8 mm plate. The ends were fabricated from thicker material in order to restrict buckle formation to the central portion of the cylinder, avoiding possible end effects. The end and central portions were rolled and welded longitudinally, giving three separate "cans". These cans were then welded together using full penetration groove welds at the butt joints. Prior to welding, the cans were arranged so that the longitudinal welds made in the first stage of fabrication were positioned 180° apart on adjacent pieces. When the three sections were welded together, the overall length of the test specimen became 2739 mm. The inside diameter of the specimen was 1753 mm throughout. Exact dimensions are listed in Table 3.1, with material properties given in Table 4.1.

3.3.2 Test Setup and Instrumentation

The test setup used for the flexural tests is shown in Fig. 3.1. It is essentially the same as that used in an earlier study (1). The setup consists of two end trusses connected to the test specimen, forming a simple beam

supported on rollers at both ends (Fig. 3.2). One end was free to translate, thus eliminating any axial restraint. Loading was applied to the truss near the connection of the specimen to the truss, so that the specimen was in pure flexure.

The specimen was connected to the truss through heavily stiffened end plates. Attachment of the specimen proceeded in stages. First, one truss and the specimen were positioned. A full penetration groove weld was made between the specimen and the end plate. Once this had cooled, the other truss was positioned and welded into place. Small gusset plates were then welded along the lower part of the specimen to end plate connection, in anticipation of the expected high tensile forces in that region.

Loading was applied through two 1800 kN capacity jacks, independently controlled through an air-powered hydraulic pump. The arrangement resulted in a maximum available moment capacity of 7950 kN·m at the test section.

Electrical resistance strain gauges were attached in three circumferential rings to the outer surface of the test specimen. One ring, at the centreline, had 16 equally spaced gauges. There were two outer rings of gauges 305 mm on either side from the centreline with 32 gauges each. Additionally, two groups of three gauges were mounted on top of the specimen, 75 mm inside the junction of the central portion and the stiffer end sections. All gauges were oriented to measure strain in the longitudinal direction.

Additional instrumentation included two 1800 kN capacity load cells, one underneath each jack. Two rotation meters were attached at the neutral axis (mid-height) of the cylinder to measure curvature of the central portion. Three displacement transducers (LVDT's) were placed inside the central portion to measure any change in inside diameter, with another three mounted outside the specimen at the neutral axis to measure vertical deflections.

3.3.3 Testing Procedure

Because the specimen was welded to a relatively stiff abutment, stresses would be induced as a result of the welding and subsequent cooling. To obtain some indication of these stresses, strains were measured before and after welding. Strain readings were also taken as the temporary central supports were removed to obtain stresses due to self weight.

The specimen was tested by increasing the jack loads in steps initially equivalent to 5% of the estimated failure load, and decreasing as this load was neared. Strain and LVDT readings were taken continually during the loading process. Rotation meter readings were taken after each load increment.

3.4 Stiffened Flexural Specimen

3.4.1 Specimen Description

The stiffened flexural specimen was constructed in a manner similar to that described in Section 3.3.1 for the unstiffened cylinder. Three portions were made and subsequently welded together. Longitudinal stiffeners were then attached.

The material used for the central portion was 5 mm thick steel meeting CSA Specification G40.21M 300W (34). The end sections were made of 8 mm thick 300W plate. The central test section was 1219 mm in length, and the end sections were each 760 mm long. The resulting overall length was therefore 2739 mm. To facilitate stiffener attachment, the outside diameter (1300 mm) was kept constant throughout.

The stiffeners were HSS 25.4 x 50.8 x 3.18, with a nominal yield strength of 350 MPa. They were attached with the narrow (25.4 mm) side contacting the cylinder, and were fastened with 5 mm intermittent fillet welds, each 50 mm in length, staggered with a pitch of 150 mm. The stiffeners were placed on the cylinder so that when the cylinder was tested, they would be on the top (compression) face. Five stiffeners were used, one at the centreline of the cross section, and two to either side, spaced at 215 mm centre to centre. This spacing corresponded to an arc of 19°, which falls into the intermediate type of a stiffened shell. The stiffener used was chosen for three reasons. The material

used was readily available, it provided great rotational restraint to the shell, and the ratio of the stiffener area to the panel area, 40%, was close to that used in other tests (22). In order that the cylinder might be more easily welded to the end plates, the stiffeners were cut 150 mm short of the end of the cylinder. This gap was filled with short portions of HSS after the connection to the end plate was completed. Exact dimensions are listed in Table 3.1, with material properties given in Table 4.1.

3.4.2 Test Setup and Instrumentation

The loading apparatus used for testing the stiffened flexural specimen was the same as that described in Section 3.3.2 for the unstiffened specimen. Attachment of the specimen to the end truss was also done in a similar fashion. One end truss and the specimen were positioned, and connected with a full penetration groove weld. The other end truss was then positioned and welded into place. After this welding was completed, small pieces of HSS 50.8 x 76.2 x 3.18 were cut and welded between the end plates and the stiffeners on the specimen to transmit compressive load directly into the stiffeners. The stiffened cylinder is shown in Fig. 3.3.

To measure strains, gauges were attached as shown in Fig. 3.3. Gauges were placed in a ring at midspan of the test section, spaced at an arc interval of 11.25° over the lower portion (below the stiffeners), and two side rings, 305 mm to either side of centreline, spaced at 22.5°. Five

bands of gauges were used on the stiffeners themselves. The three central rings were continued on top with each ring having three gauges on each stiffener and two on the shell between stiffeners. On the stiffener, one gauge was mounted on the top face, and one at midheight (25 mm) on either side. Gauges between stiffeners were placed 50 mm from the edge of the stiffener. Additionally, two partial rings were placed on the central test section 75 mm from the welds joining the centre and end sections. These consisted of one gauge on top of each stiffener, and two to either side of the top stiffener. A total of 141 gauges were used.

To measure load, two 1800 kN capacity load cells were placed under the jacks. Three LVDT's were placed inside the centre portion of the specimen to measure changes in the inside diameter during loading, and another three were placed at midheight on the outside to measure the vertical deflection. Two rotation meters were mounted at the ends of the central test section of the specimen to obtain a measurement of the curvature.

3.4.3 Testing Procedure

As described in Section 3.3.3 for the unstiffened cylinder, strain readings were taken before and after welding, and during removal of the temporary central supports to obtain strains due to welding and self weight.

During the test, the load was increased in steps initially equivalent to about 5% of the estimated failure load,

and decreasing as the ultimate load was approached. Strain gauge and LVDT readings were taken continually during loading. Rotation meter readings were taken at the end of each load step.

3.5 Shear Specimens

3.5.1 First Shear Specimen (R/t = 251)

3.5.1.1 Specimen Description

The first shear specimen was constructed from five pieces of cold-rolled steel sheet welded flat, rolled to shape, and completed by making a single longitudinal seam weld. All welds were full penetration groove welds made by the manual shielded metal arc process, using E410 electrodes.

After the longitudinal seam weld was completed, two collars of 6 mm plate, 50 mm wide, were welded inside each end in order to provide a heavier base for attachment of the specimen to the end plates. These rings were connected with a fillet weld.

The configuration of the specimen is shown in Fig. 3.4. The middle and end portions were made from 16 gauge (1.52 mm) material, with the two test sections made from 22 gauge (0.76 mm) material. All material was cold-rolled sheet steel, oriented such that the rolling direction of fabrication was parallel to the longitudinal axis of the specimen. Exact dimensions are listed in Table 3.1, with material

properties given in Table 4.1.

3.5.1.2 Test Setup and Instrumentation

The first step in test preparation was to place strain gauges on the specimen so that strains could be measured during subsequent steps. Next, the specimen was attached to 25 mm thick end plates. This was accomplished with a fillet weld between the end plate and the 6 mm thick ring, with the specimen in a vertical position. The specimen was then placed between two columns bolted to the floor, leaving a gap of about 5 mm at each end. Bolts were placed between the end plates and the columns, and a high strength grout was then poured between the column and end plates. This was necessary because the end plates had warped slightly during welding and did not fit flush against the column. Once the grout had set, the bolts were tightened, and additional clamps were placed to further fix the ends.

Loading was accomplished with a 450 kN capacity hydraulic jack, operated with a hand pump. To simplify the test setup, the jack was placed between the specimen and the floor, thus loading the specimen upwards.

The jack load was transmitted to the specimen through a cradle around the bottom 80° of the cylinder. The cradle gave a two point load, 145 mm between load points. Plaster of Paris was placed between the cradle and the specimen to obtain even bearing. In order that the central portion would not be crushed locally, circular plywood diaphragms 19 mm thick were placed inside the specimen at the loading points.

The jack load was measured with a 90 kN capacity load cell between the cradle and the jack. Deflections were measured using four LVDT's. One was at the centre, above the jack, and the other three were at either end and the centre of one of the shear spans.

Strains were measured using two rings of electrical resistance strain gauge rosettes. Each rosette consisted of one gauge mounted parallel to the longitudinal axis, one perpendicular, and a third at 45° between the others. These rings were placed at the theoretical points of inflection, mid-way along the shear spans. One ring consisted of rosettes evenly spaced at a 45° arc length, and the other ring spaced at 90°. In the latter case, the first gauge was 45° from the top of the specimen.

Additional gauges were mounted top and bottom near the transition welds between the thin shear spans and the thicker centre and end portions, in order to monitor the bending behaviour at those points.

3.5.1.3 Testing Procedure

Strains were monitored when the specimen was being bolted to the columns. It was observed that when the bolts were tightened when the end plate was directly contacting the column, strains of approximately 10% of the yield strain were induced in the near shear span. To overcome this, a gap was left between the end plate and the column, which was then filled with a high strength grout. After the grout had cured, the bolts were retightened, and strains were again

monitored. It was found that no significant strains occurred when this system of connection was used.

Because all instrumentation was read remotely by a data acquisition system, there was no need to stop the test to manually read gauges. Hence, loading was performed continuously, monitoring the load and deflection all the while. Loading was stopped temporarily when buckles occurred. The buckles were marked and the load recorded before continuing. This process continued until the maximum load was reached.

3.5.2 Second Shear Specimen (R/t = 75)

3.5.2.1 Specimen Description

The second shear specimen was fabricated from ASTM A36 grade steel. The specimen configuration was similar to the first shear specimen, and is shown in Fig 3.5. The two shear spans, each 762 mm in length, were made from 5 mm plate. The two end sections, each 355 mm in length, and the central loading portion, 1091 mm in length, were made from 8 mm plate. When the five sections were welded together, the overall length of the test section was 3295 mm. The outside diameter of the specimen was 762 mm throughout. The fabrication of the specimen was done in a manner similar to that described in Section 3.3.1 for the unstiffened cylinder tested in flexure. Five separate "cans" were made and subsequently welded together using full penetration groove welds. Prior to welding, the cans were arranged so that the longitudinal welds were positioned 180° apart on adjacent pieces.

Exact dimensions are listed in Table 3.1, with material properties given in Table 4.1.

3.5.2.2 Test Setup and Instrumentation

The test setup used for the large diameter shear test is shown in Fig. 3.6. It consisted of the specimen placed between two sets of columns, with the load applied upwards at the centre of the specimen. Before the specimen was placed into the testing position, two pieces of 50.8 x 76.2 x 3.18 HSS were placed vertically inside the cylinder, in order to reduce the ovaling of the cross-section at the point of loading. The loading system was designed to prevent buckling at the point of loading. It consisted of two 20 mm plates, each having a cutout in the shape of a semicircle of diameter equal to that of the cylinder. These plates were placed around the cylinder, and welded to it. The result was a diaphragm encircling the cylinder at the point of loading. This was done at two load points, each 175 mm to either side of centre. A 25 mm plate was attached to the bottom (loading) edge of the diaphragms, connecting them to each other. This was intended to reduce the possibility of sideways movements of the diaphragms.

The end fixtures of the setup consisted of two sets of three columns placed side by side, bolted together, and to the floor of the testing area. The two sets were joined at the top by tension rods. End plates having a thickness of 25 mm were bolted to the column sets, and the specimen was positioned and welded to the end plates. The bolts

connecting the end plates to the column and those connecting the columns to the floor were left loose during welding, so that shrinkage stresses were minimized. After cooling, the end plate bolts were tightened, and then the floor bolts were tightened. Longitudinal strain gauges mounted on the specimen were monitored during this process, and it was found that no significant strains occurred.

Loading was applied through two 1800 kN capacity jacks, independently controlled through an air-powered hydraulic pump. A 900 kN capacity load cell and a ball and socket joint were placed between the jacks and a bearing plate below the diaphragms.

Electrical resistance strain gauges were attached to one of the test sections in order to monitor bending strains during loading. Deflections were measured with four LVDT's. One was at the centre of the specimen, and the other three were at either end and at the centre of one of the shear spans.

3.5.2.3 Testing Procedure

The loading procedure for the large diameter specimen was similar to that for the small diameter specimen described in Section 3.5.1.3. Loading was performed continuously, with a remote data aquisition system recording the data.

Table 3.1 Specimen Geometry

Test	Material	Radius[1] mm	Length mm	Thickness mm	R/t	L/R	Remarks
Unstiffened flexural	700Q	879.0 (880.5)[2]	1219 (760)	5.05 (7.94)	174.1 (110.9)	1.39 (0.86)	Thickened tubular sections at ends.
Stiffened flexural	300W	647.5 (646.0)	1219 (760)	5.05 (7.94)	128.2 (81.4)	1.88 (1.18)	Thickened tubular sections at ends. Longitudinal stiffeners are 50.8 x 25.4 x 3.18 HSS.[4]
Shear #1	Sheet	190.4 (189.7)[3]	381 (165)	0.76 (1.52)	250.5 (124.8)	2.00 (0.87)	Shear specimens have two test spans in each specimen. Values given are for a single test span. Thickened tubular sections at ends and at centre.
Shear #2	A36	378.5 (377.0)	762 (355)	5.05 (7.94)	75.0 (47.5)	2.01 (0.94)	

1. Radius of middle surface.
2. Numbers in parentheses refer to values for end sections.
3. Numbers in parentheses refer to values for end sections, and for central loading section from loading point to shear span.
4. Measured dimensions of HSS are 50.85 x 25.62 x 3.324. Calculated area = 435.5 mm^2

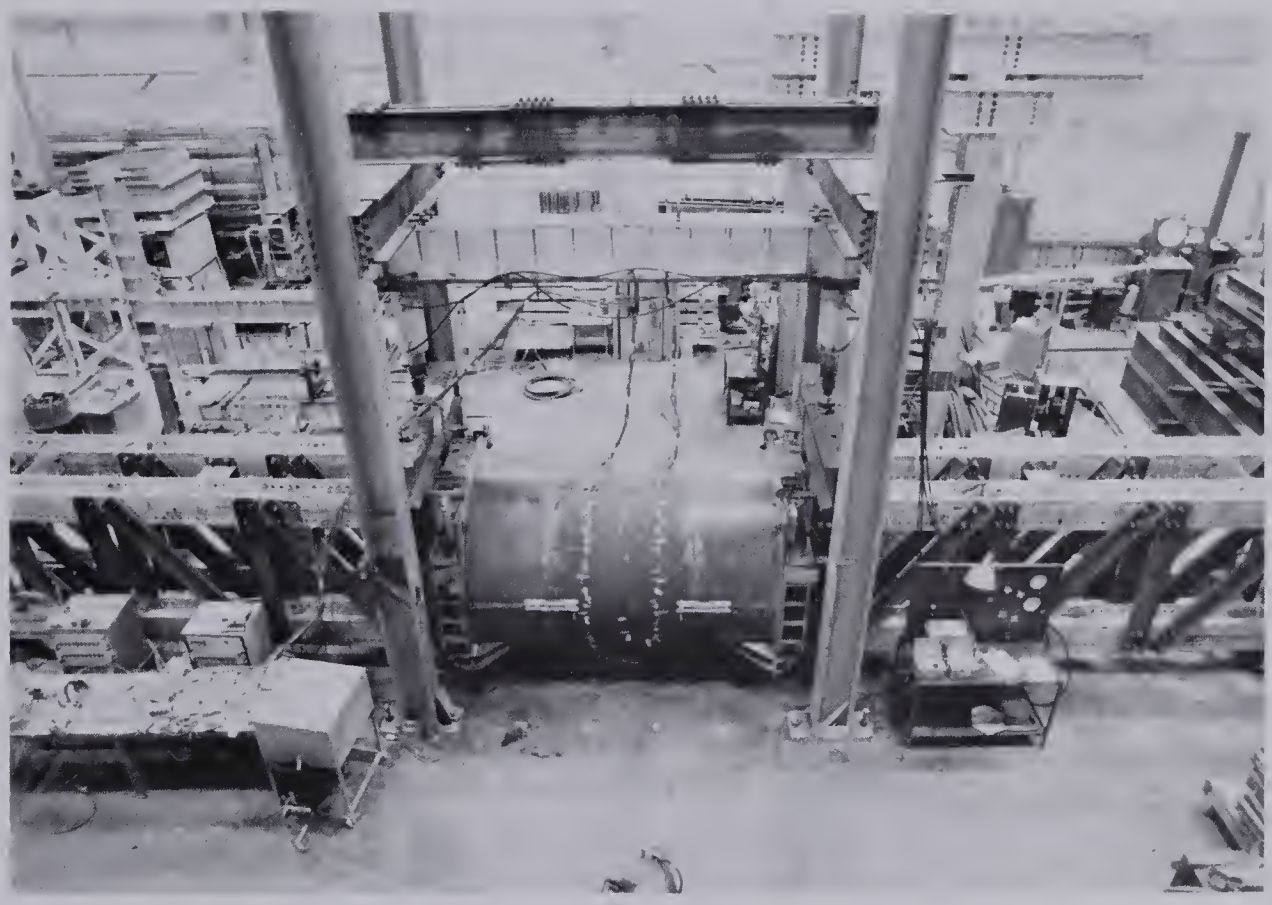

Figure 3.1 Bending Apparatus, Unstiffened Specimen

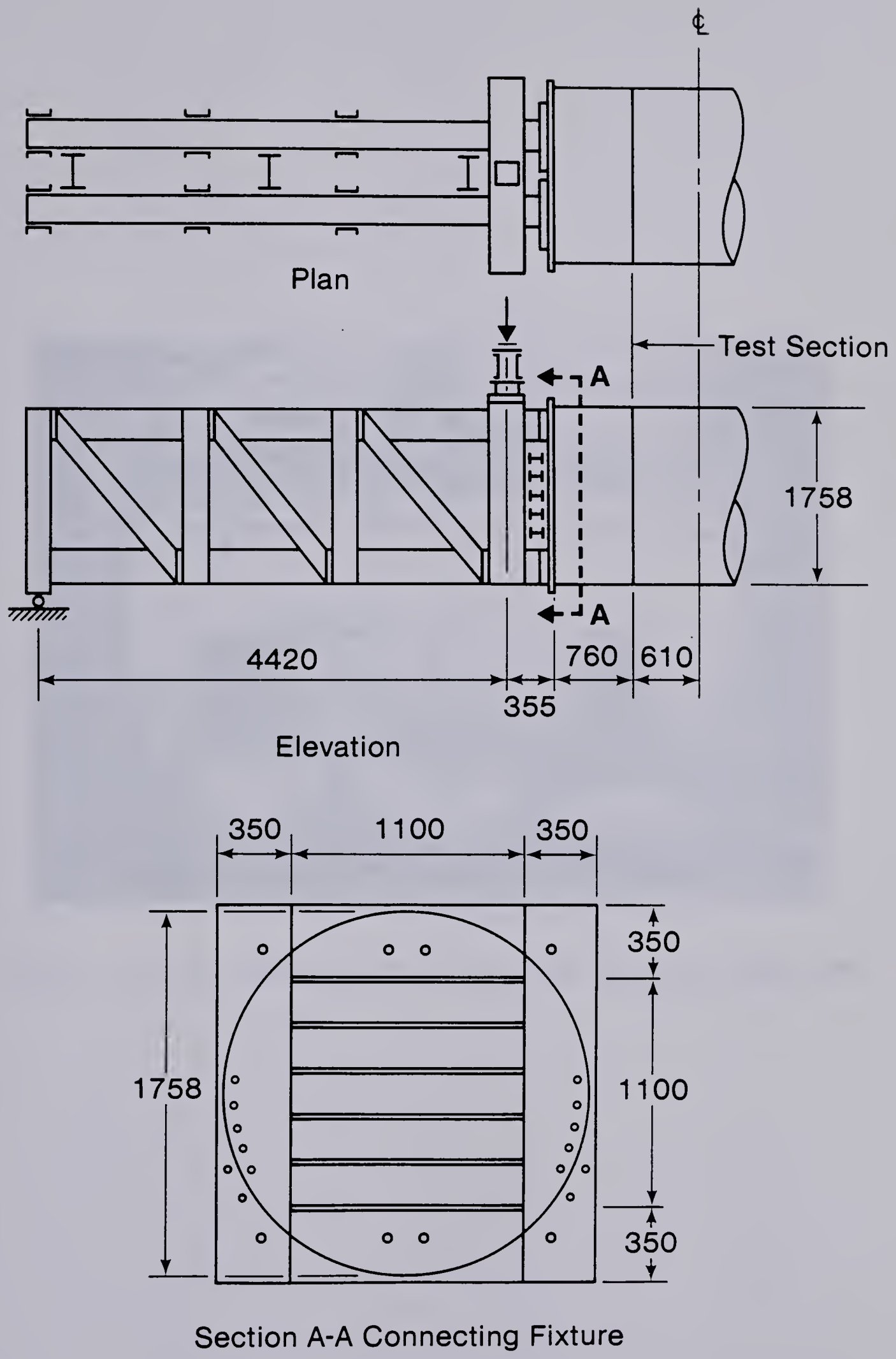

Figure 3.2 Composite Beam Used in Bending Tests

Figure 3.3 Instrumentation, Stiffened Flexural Specimen

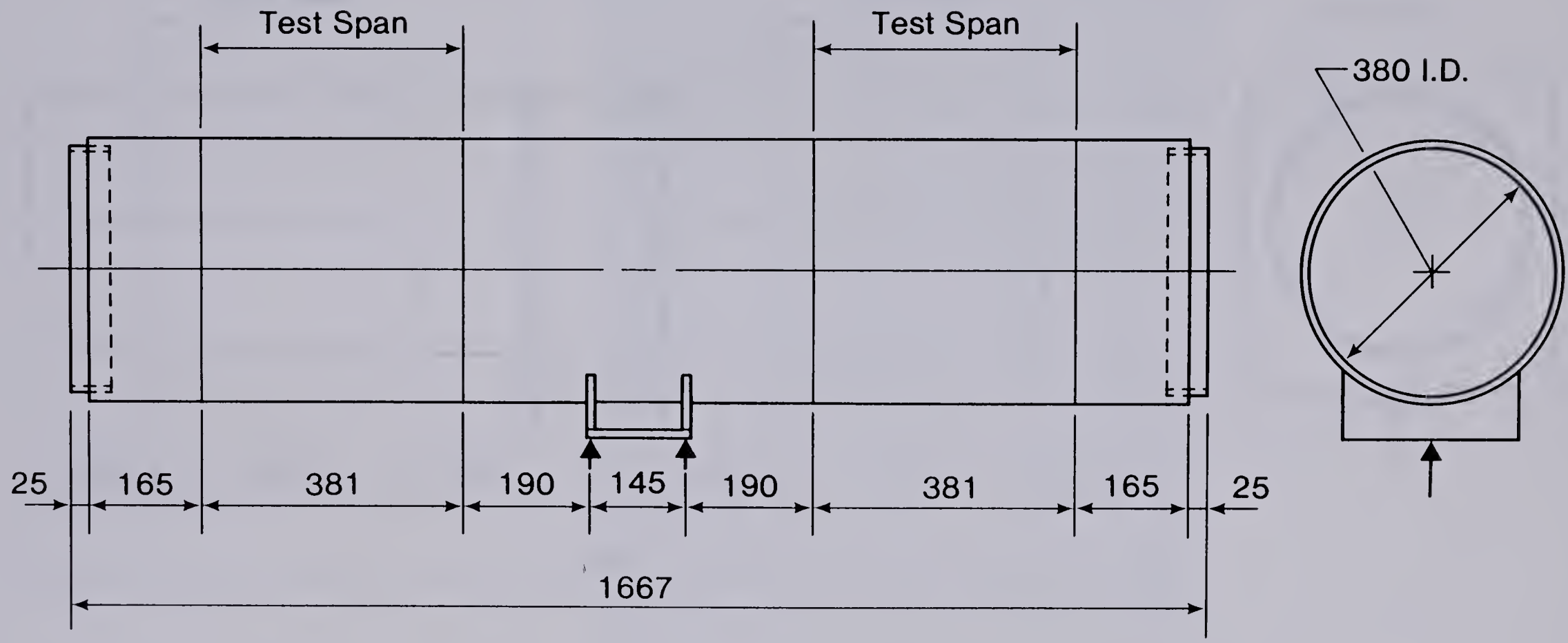

Test Spans: t = 0.76 mm

Other Spans: t = 1.52 mm

Figure 3.4 First Shear Specimen Configuration

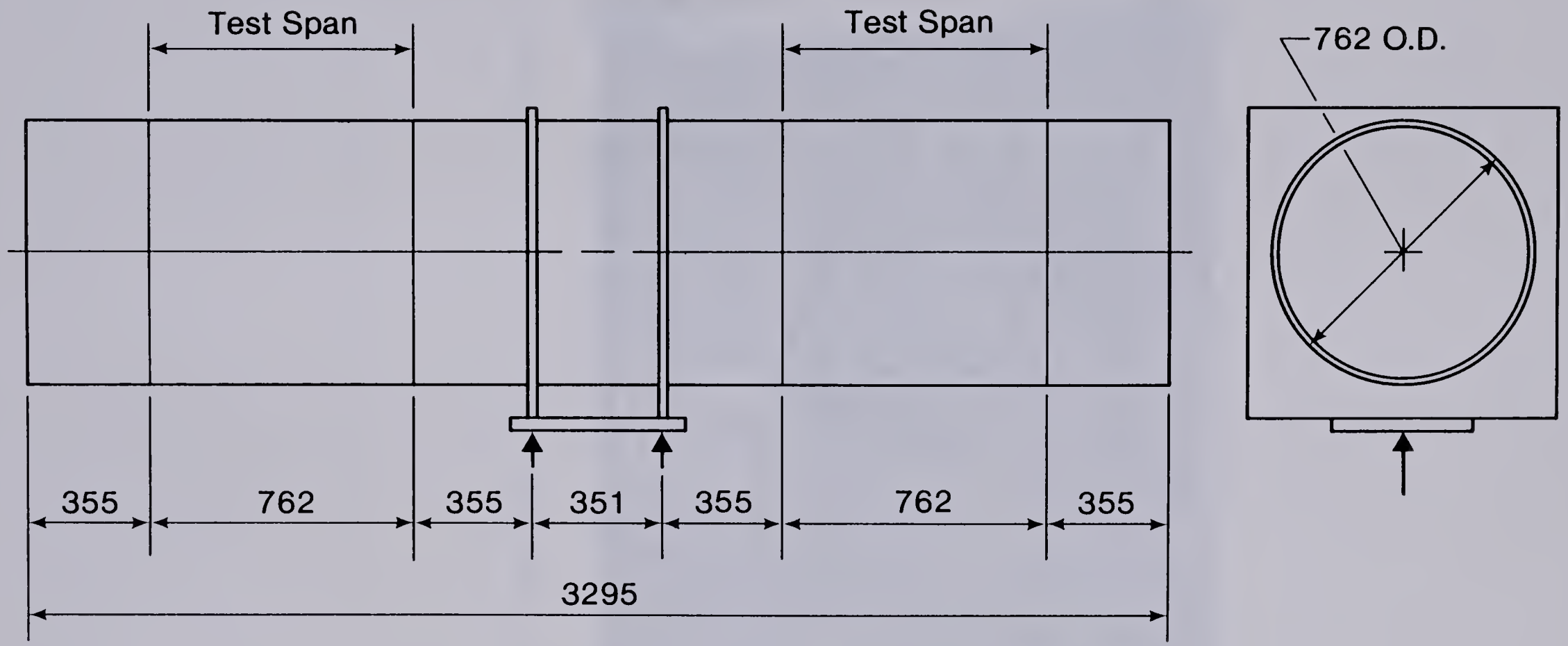

Test Spans: t = 5.05 mm

Other Spans: t = 8 mm

Figure 3.5 Second Shear Specimen Configuration

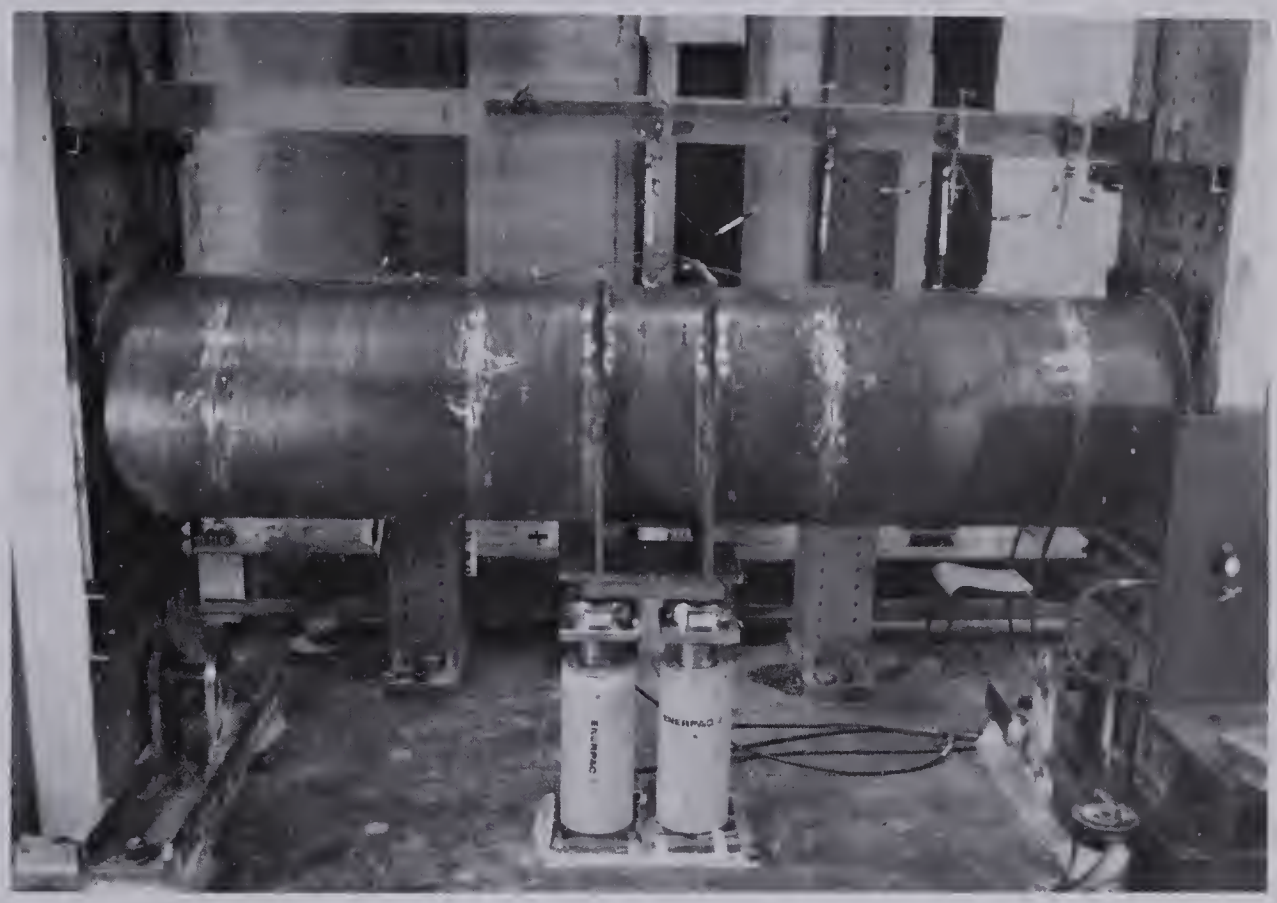

Figure 3.6 Second Shear Specimen Test Setup

4. Experimental Results

4.1 Introduction

The results of the experimental program are presented in this chapter. In Section 4.2 the methods used for determining the material properties of the test specimen material are presented. Section 4.3 describes the loading behaviour and the results of the test of the unstiffened flexural specimen. A description of the stiffened flexural test is presented in Section 4.4, and Section 4.5 describes the results of the two shear tests.

4.2 Material Properties

Table 4.1 lists the modulus of elasticity values, the static yield point, and Poisson's ratio, as determined from tensile tests on coupons taken from the plate material used in the test specimens. Four coupon tests were performed in each case, and the average values are reported, along with the maximum deviations from the mean.

The modulus of elasticity and Poisson's ratio were determined from strains measured by strain gauges mounted parallel and perpendicular to the direction of loading on two coupons of each test specimen material. Strain readings were taken at intervals during loading in the linear region, and a best fit line was used to calculate the modulus of elasticity. Poisson's ratio was taken as the average value of the transverse strain over the longitudinal strain.

The yield value reported for the hollow structural shape used as stiffeners is the average determined from three tests on 100 mm long stub columns. Yield values were calculated by the 0.2% offset method.

4.3 Unstiffened Tube Bending Test Results

4.3.1 General Observations

The specimen failed by local buckling at a load less than that theoretically required to produce yielding. Depressed diamond shaped buckles formed in the compression region of the central test section adjacent to one of the circumferential welds joining the test section to the end section. The buckles covered approximately the top 3/7 of the circumference, and were approximately symmetric about the extreme top fibre. A portion of the buckled shape of the specimen is shown in Fig. 4.1.

4.3.2 Behaviour During Loading

The behaviour of the specimen is shown in Fig. 4.2 where a plot of the moment versus curvature response of the central test section is presented. The curvatures plotted are those derived from strain gauge readings, rotation meter readings, as well as a theoretical curve obtained using linear elastic beam theory.

The curvature calculated from the longitudinal strain gauge readings is the average curvature determined from the

difference in measured strain between the extreme compression and tension regions.

The curvature obtained from the rotation meter readings was calculated from the change in slope between the meters attached to either end of the central test section at the neutral axis. The value given is the change in slope between the two gauges, divided by the distance between them. This accounts for any end settlements, and for the length of the test section.

The specimen behaviour was practically linear up to the failure moment of 4253 kN·m. Flattening of the cross-section, as determined by change in the vertical diameter, reached a maximum of 5.9 mm just prior to failure. This corresponds to 0.34% of the initial diameter.

The buckling failure was very sudden, all buckles apparently being formed simultaneously. The whitewash applied prior to testing gave no indication that local yielding occurred prior to failure. The moment at failure of 4253 kN·m corresponds to an extreme fibre stress of 349 MPa, based on elastic beam theory. The cross-sectional longitudinal strain distribution, as determined from strain gauge readings, is shown in Fig. 4.3.

It can be seen that the strain distribution is not linear, and that the curvature calculated from the strain gauge readings is approximately 12% in excess of that calculated from the curvature gauges and elastic beam theory, see Fig. 4.2. This nonlinearity of strain distribution helps to

account for the large variation between the curvatures, as the curvature calculated from the strain gauges assumed that plane sections remain plane, which was not observed in this case. Possible reasons for the nonlinear strain distribution are first, the connecting fixtures may have been overloaded, causing a change in the rigidity of the system, and second, the existence of membrane stresses in the shell. These would tend to cause transverse tensile strains in the top of the cylinder, and transverse compressive strains in the lower region. This difference may change the cross-sectional strain distribution, but no theoretical analysis has been performed for this load case.

The maximum measured strain occurred just before failure, and corresponded to a compressive stress of 407 MPa, which is approximately 17% greater than that predicted by elastic beam theory. When the initial stresses resulting from welding and specimen dead weight are added, the total compressive stress at failure was 419 MPa, or 20% in excess of that calculated by elastic beam theory.

4.4 Stiffened Tube Bending Test Results

4.4.1 General Observations

The specimen failed by yielding of the shell, leading to buckling. Considerable post-buckling strength was observed, with the maximum load obtained approximately 1.8 times the load at first yielding. Buckles formed over the

entire compression region of the central test section, with buckles in the regions of highest stress having the greatest amplitude. A portion of the buckled shape is shown in Fig. 4.4.

4.4.2 Behaviour During Loading

The behaviour of the specimen is shown in Fig. 4.5 where a plot of moment versus curvature of the central test section is presented. The curvatures are derived from strain gauge readings, and rotation meter readings. A theoretical curve derived using linear elastic beam theory is also shown.

The curvature calculated from the longitudinal strain gauge readings is the average curvature determined from the difference in measured strain between the extreme compression and tension regions.

The curvature calculated from the rotation meter readings was calculated from the change in slope between the meters attached to either end of the central test section at the neutral axis. The value given is the change in slope between the two gauges, divided by the distance between them.

The behaviour of the specimen was practically linear up to a moment of about 1700 kN·m. At about 1750 kN·m, local yielding occurred on the top compression face of the shell near the end plates. The whitewash flaked off in lines angled at approximately 45° to either side of the top

stiffener. This yield pattern increased slightly in size until about 2200 kN·m, at which point a small transverse crease appeared, extending between two stiffeners at the centre of the test span, between two stitch welds. Another crease appeared next to this one at a moment of about 2400 kN·m. At about 2600 kN·m, the topmost stiffener began to buckle along with the shell underneath. The stiffener and the shell buckled downwards. This buckle occurred at the location of the first crease. As loading progressed, the existing buckles increased in amplitude, and further buckles formed. The specimen was judged to have failed when the moment versus curvature behaviour became nonlinear. This would be a serviceability limit state. The actual ultimate capacity of the test section would occur when further extension of the jacks would produce no additional increase in load. However, this was unobtainable because the vertical deflection of the specimen ($\simeq$ 110 mm) was so large as to approach the capacity of the testing apparatus. However, at the end of the test, the load versus deflection behaviour was practically horizontal, signifying the approach of a maximum load.

The maximum moment reached was 3068 kN·m. This is about 88% of the theoretical fully plastic moment capacity. Average strain distribution over the cross-section at various load increments for gauges on the specimen's east face is shown in Fig 4.6. The yield strain shown (0.00167) is that obtained by dividing the maximum stress, taken to be the

value of σ_{y_s} (338 Mpa), divided by the modulus of elasticity (202 900 MPa), see Table 4.1.

4.5 Shear Test Results

4.5.1 First Shear Test

4.5.1.1 General Observations

The specimen failed as a consequence of a series of inclined buckles forming in the shear spans, after which no further load could be applied. The buckles were all at about the same angle, 24°, relative to the longitudinal axis, and approximately symmetric about both the longitudinal axis and the centre of the specimen. Fig. 4.7 shows the buckle patterns on the sides.

4.5.1.2 Behaviour During Loading

The specimen behaviour during loading is shown in Fig. 4.8, where a plot of load versus the vertical deflection at the centre of the test specimen is presented. The load given is that on one shear span, which is half the actual jack load. The behaviour is practically linear up to a load of about 22.5 kN, at which point the first buckle formed. The load dropped off, but picked up again. At about 26 kN, another buckle formed, on the specimen face opposite the first one, the load again dropping. At about 26.5 kN, it was necessary to unload the specimen in order to make adjustments to the loading apparatus. The plywood of the

loading cradle was being crushed at the jack, and a metal plate was therefore inserted. No further problems occurred. The buckles did not change in appearance during the unloading or subsequent reloading. The reloading path followed the unloading path very closely. The behaviour became substantially non-linear at a load of about 28 kN. At this point, buckles started to form quickly, with deflection increasing rapidly as well. A maximum load of 29.4 kN was reached, and thereafter no further load could be applied to the specimen.

4.5.2 Second Shear Test

4.5.2.1 General Observations

The specimen failed after inclined buckles had formed in one shear span, after which no further load could be applied. The span that failed had buckles approximately symmetric about the longitudinal axis. The other span showed no visible evidence of failure. The buckled shape is shown in Fig. 4.9.

4.5.2.2 Behaviour During Loading

The specimen behaviour during loading is shown in Fig. 4.10 where a plot of load versus the vertical deflection at the centre of the test specimen is presented. The behaviour is practically linear up to a load of about 750 kN, and then starts to curve until the maximum load of 967 kN is reached. At this point the first buckle formed, causing the load to

drop off rapidly, to 880 kN. The second buckle formed soon after, at 890 kN, at which point the load again dropped, to about 750 kN. Further extension of the jacks increased the amplitude of the buckles, although no further buckles formed, and produced a small decrease in load, until a plateau of about 660 kN was reached. The loading was stopped at two points to make a visual inspection of the test apparatus. The load dropped off slightly during these inspections, but was regained upon continued loading.

Table 4.1 Material Properties

Test	Material	E MPa	σ_{ys} MPa	ν
1. Unstiffened flexural	700Q (1)	202 400	729 (4) (+10,-15)	0.27
2. Stiffened flexural (shell)	300W (1)	202 900	338 (+7,-10)	0.26
(stiffeners) (0.2% offset)	HSS (2)	-------	531 (+22,-15)	----
3. Shear #1	Plate (3)	204 400	301 (+9,-13)	0.33
4. Shear #2	A36	196 400	308 (+28,-18)	0.28

1. According to CSA G40.20M-1977.
2. Hollow Structural Shapes.
3. Cold-rolled sheet.
4. Values in parentheses are the maximum and minimum deviations from the mean value.

Figure 4.1 Buckled Shape of Unstiffened Flexural Specimen

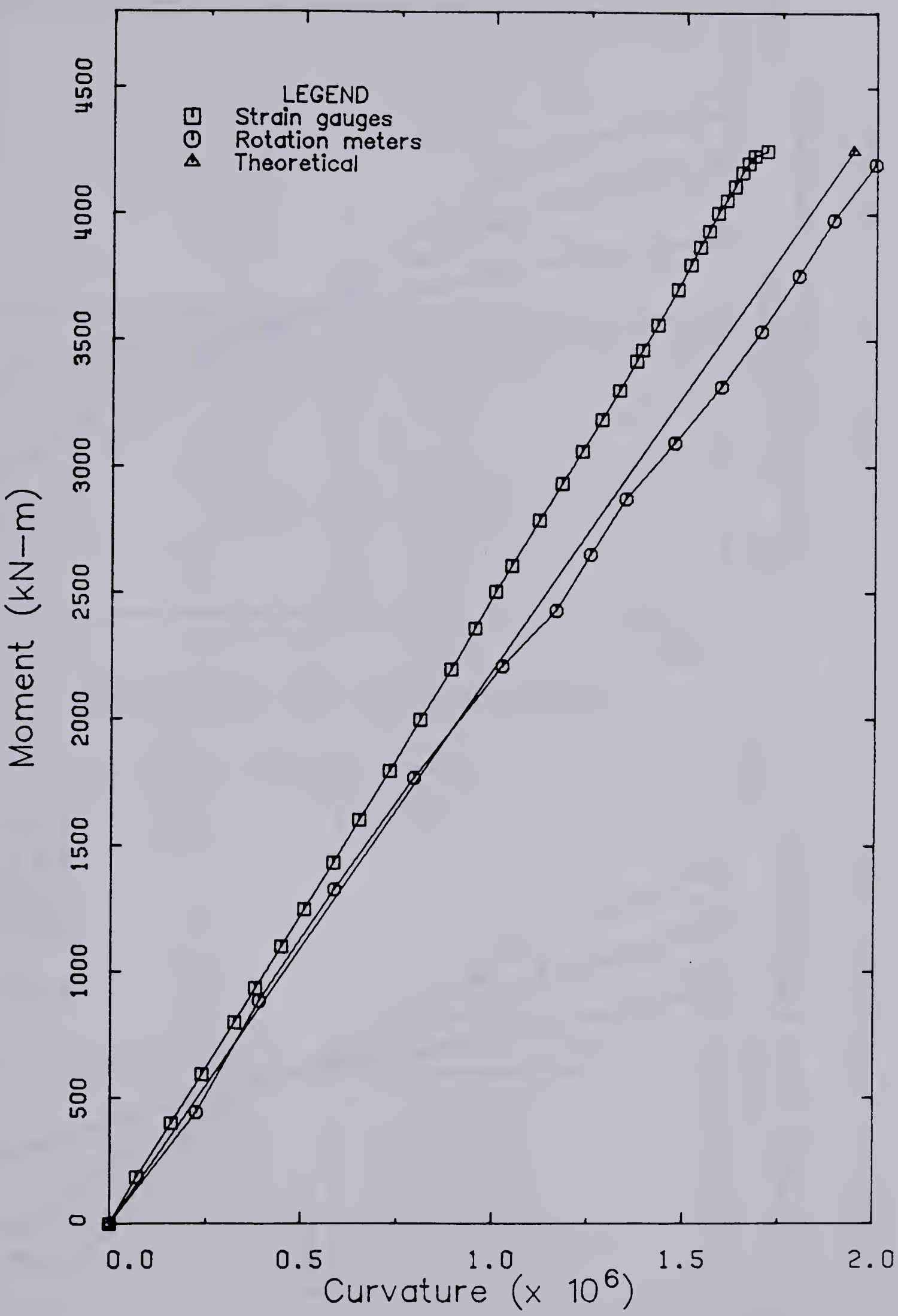

Figure 4.2 Moment-Curvature Behaviour of Unstiffened Flexural Specimen

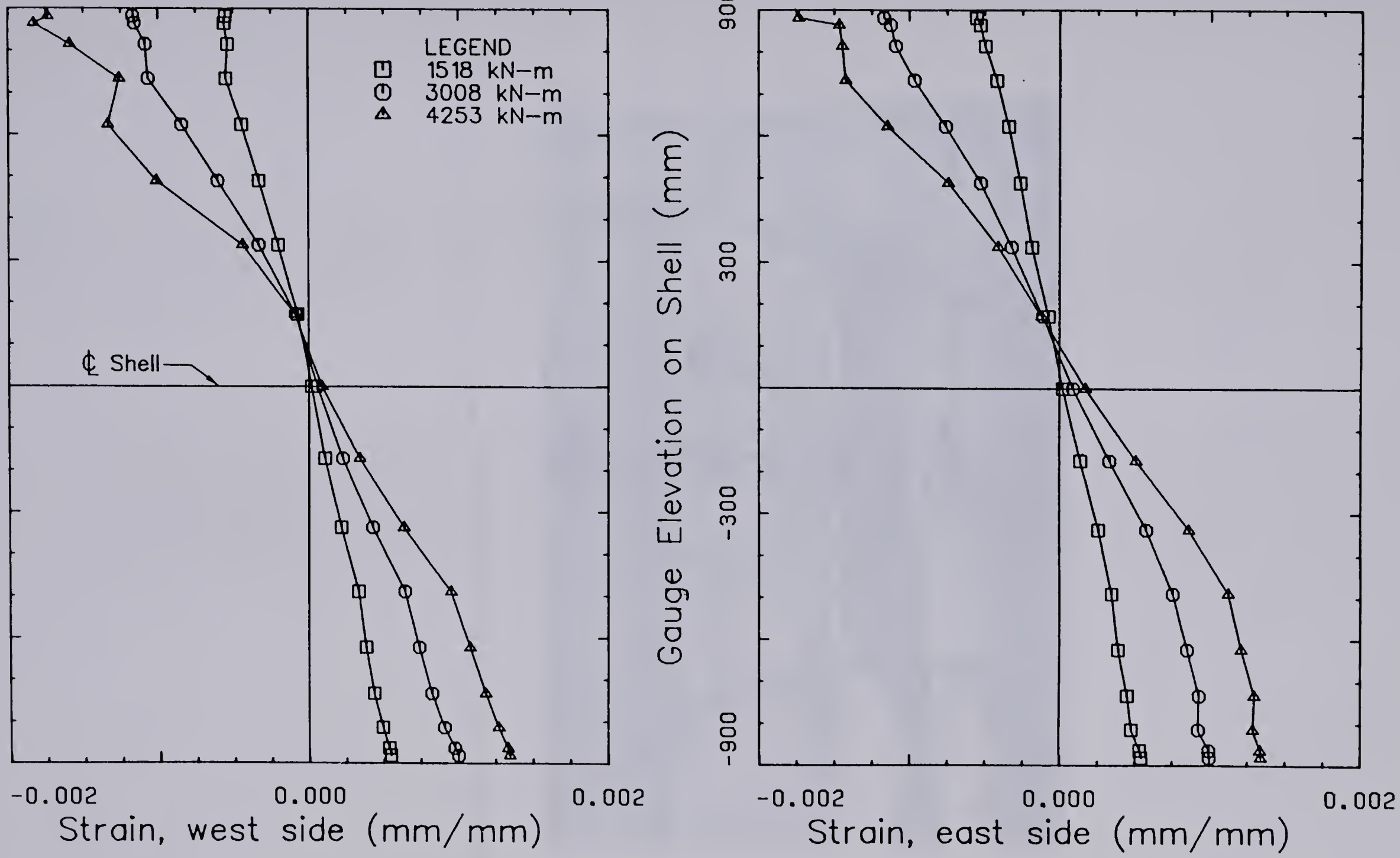

Figure 4.3 Longitudinal Strain Distribution in Unstiffened Flexural Specimen

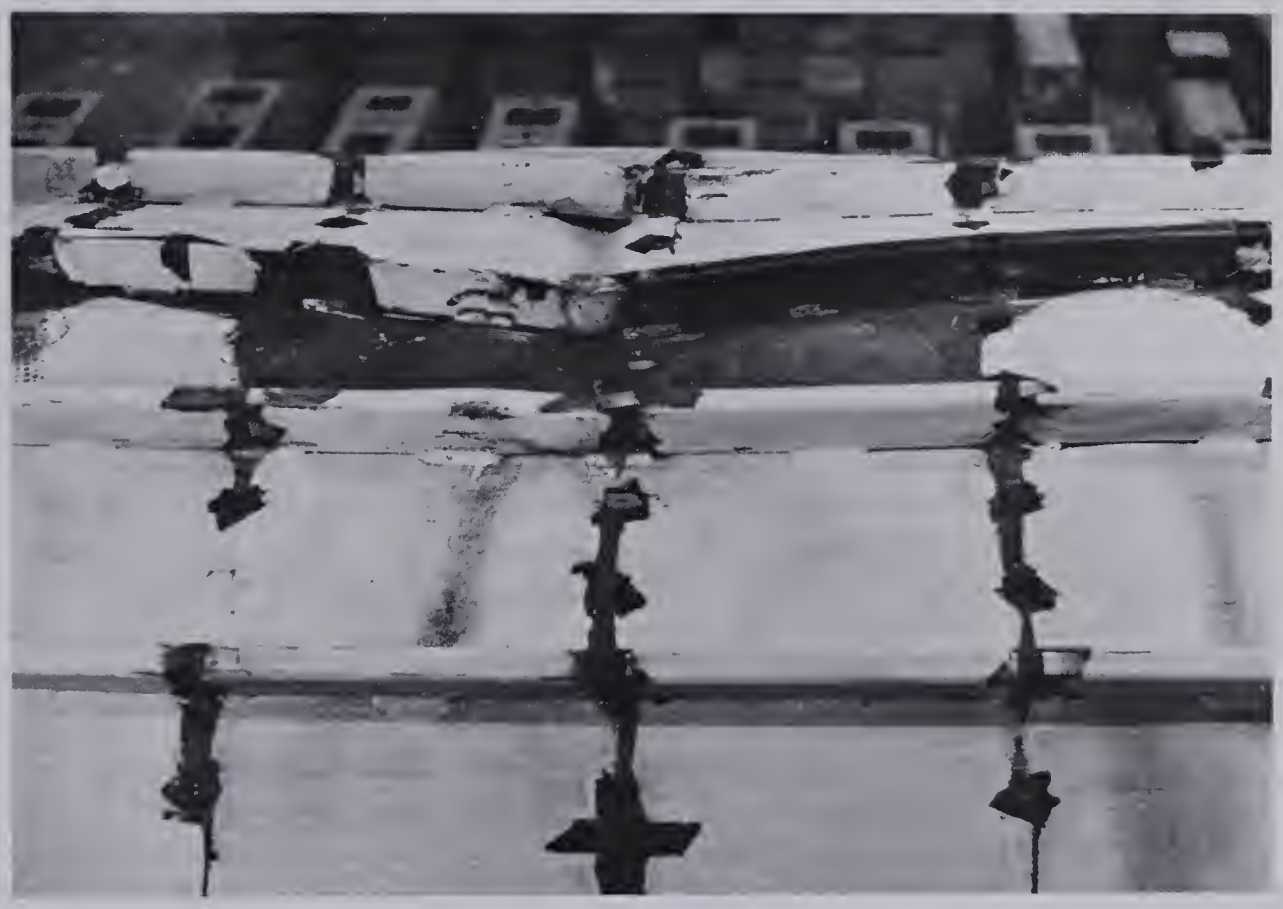

Figure 4.4 Buckled Shape of Stiffened Flexural Specimen

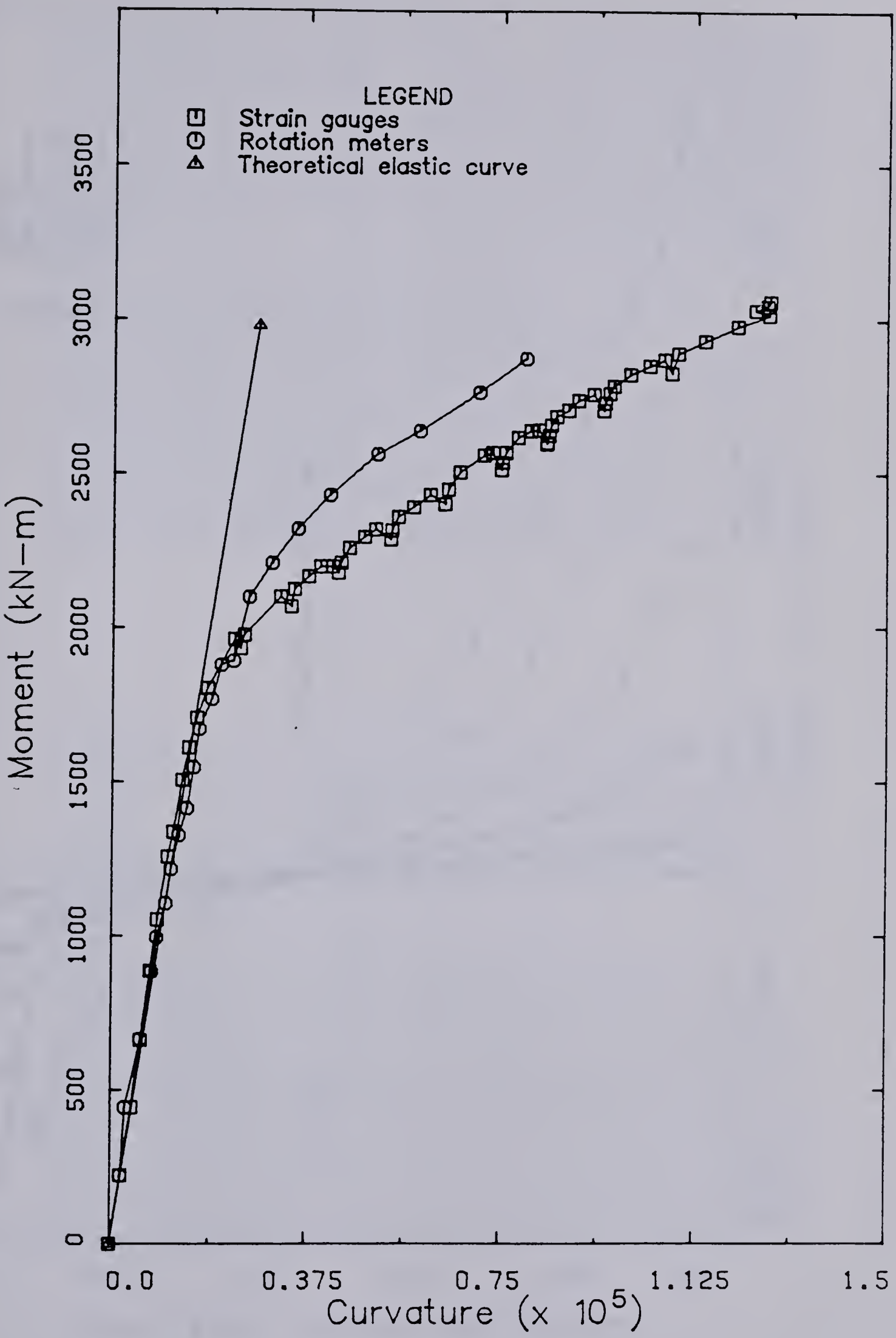

Figure 4.5 Moment-Curvature Behaviour of Stiffened Flexural Specimen

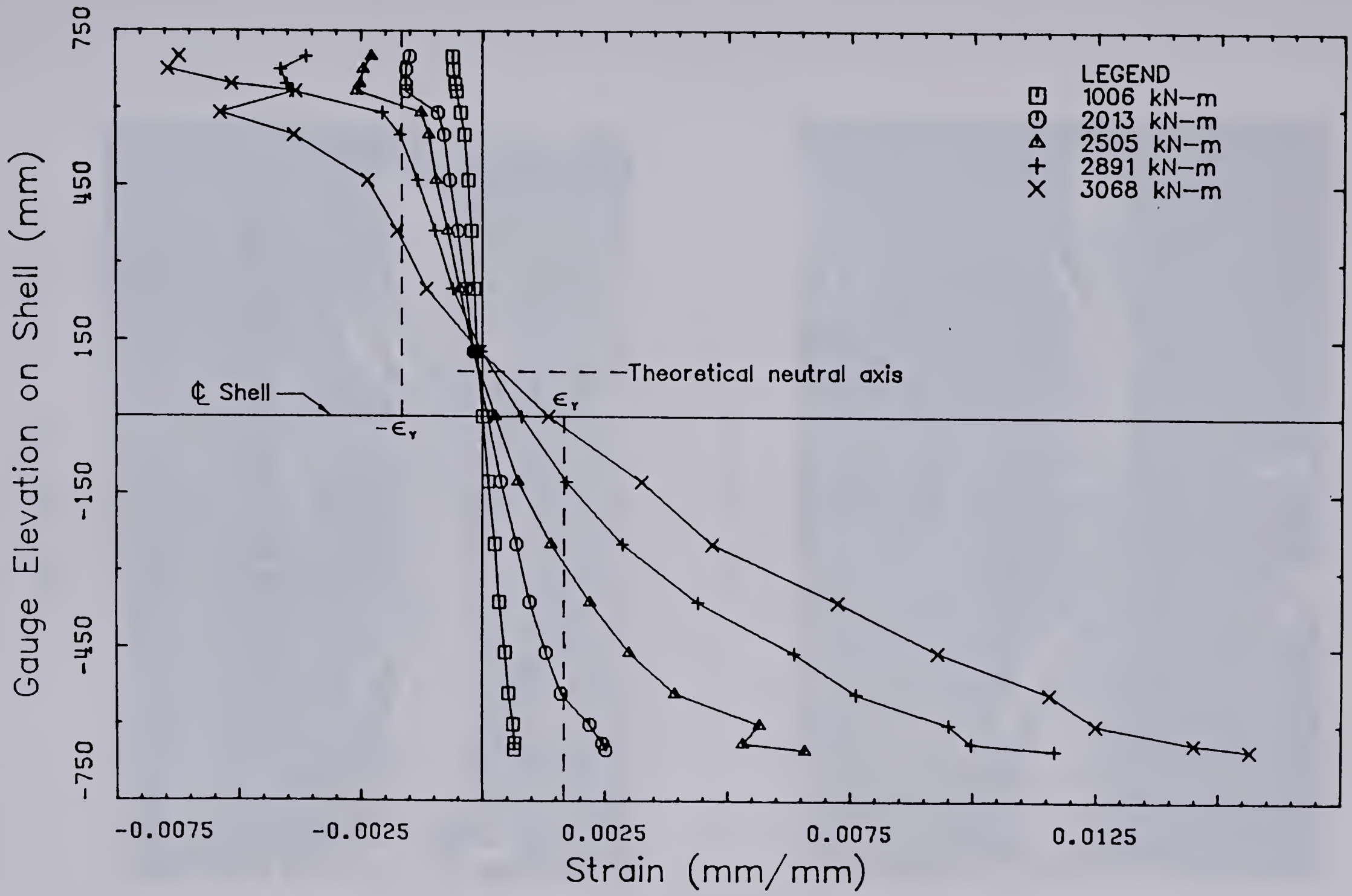

Figure 4.6 Longitudinal Strain Distribution in Stiffened Flexural Specimen

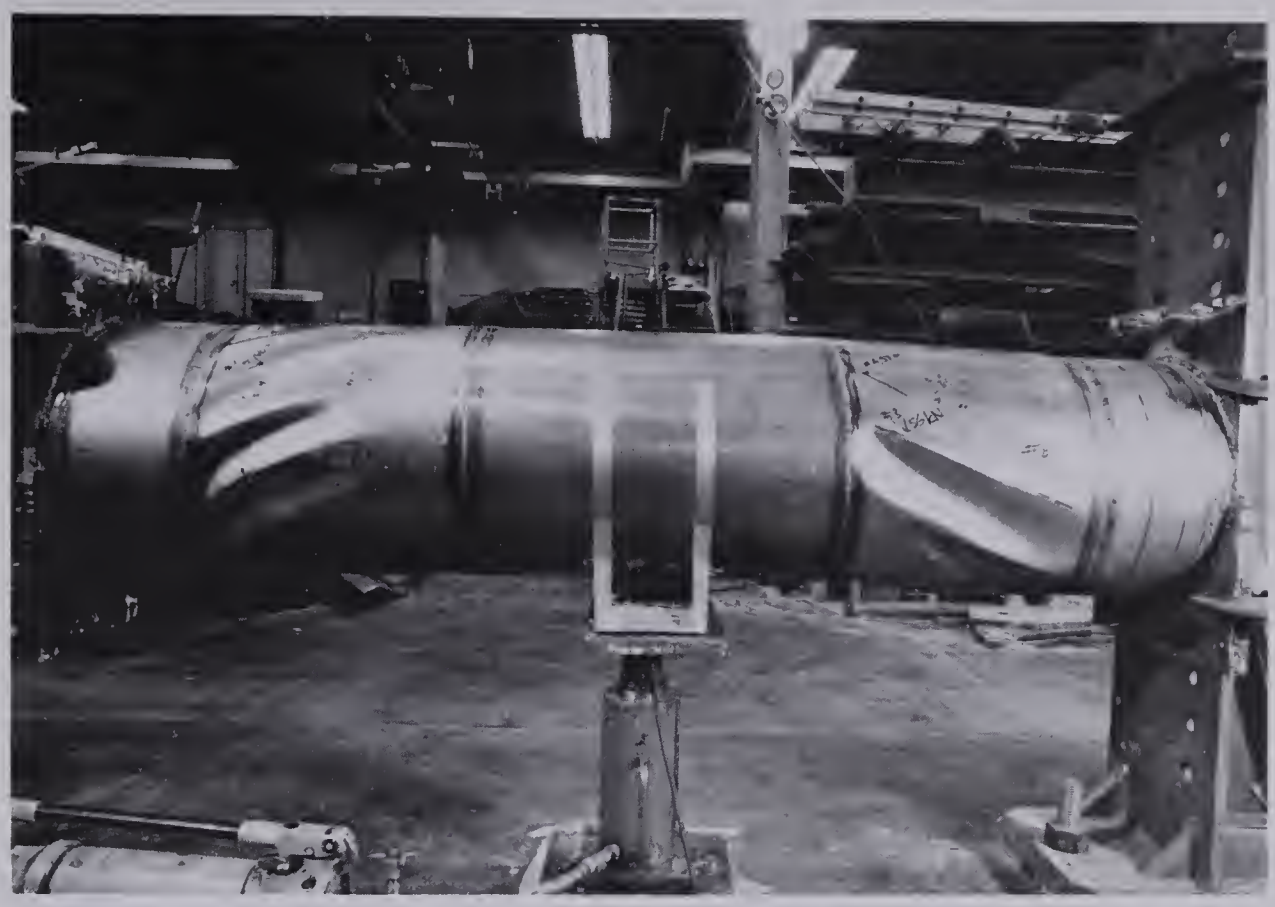

(a) East Face

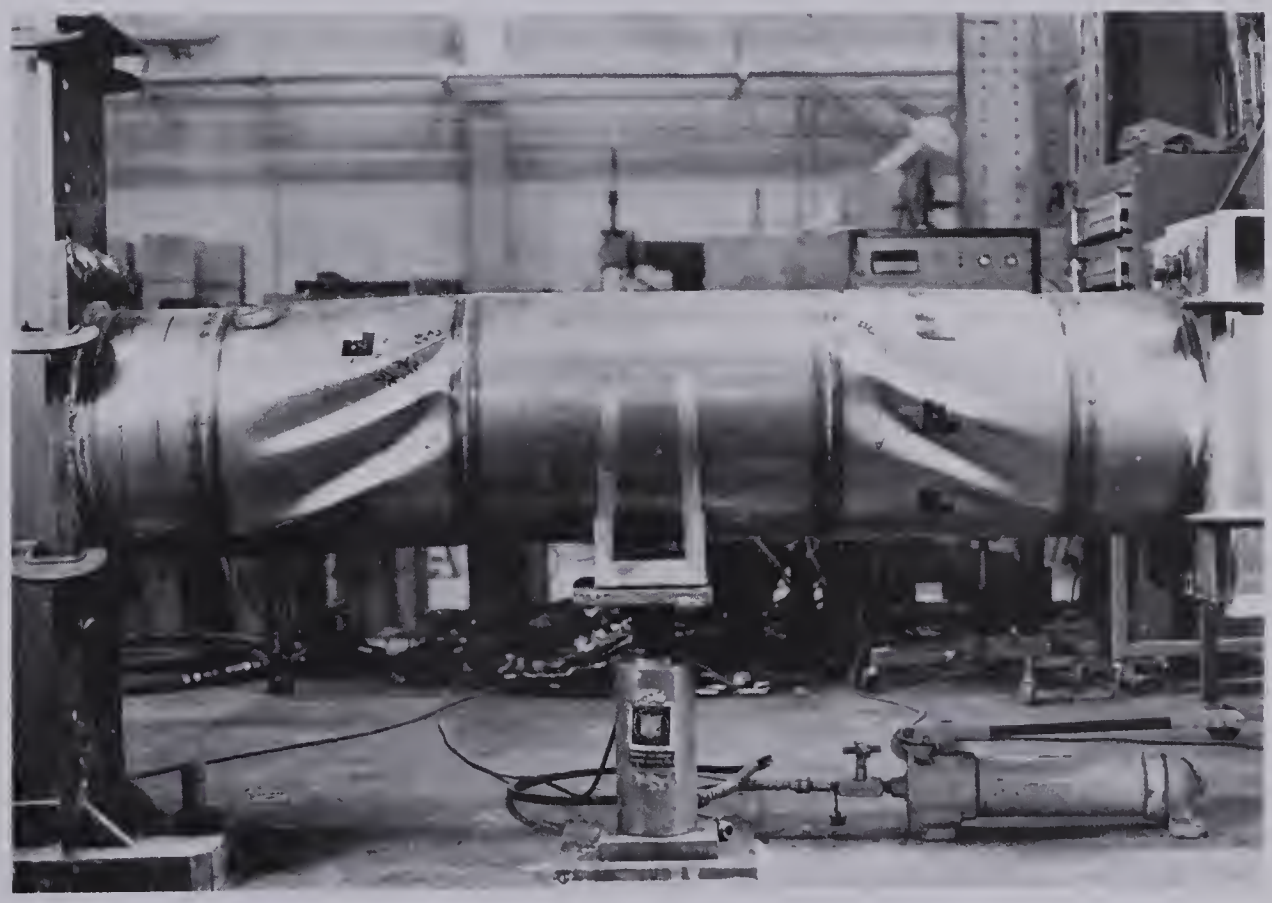

(b) West Face

Figure 4.7 Buckled Shape of First Shear Specimen

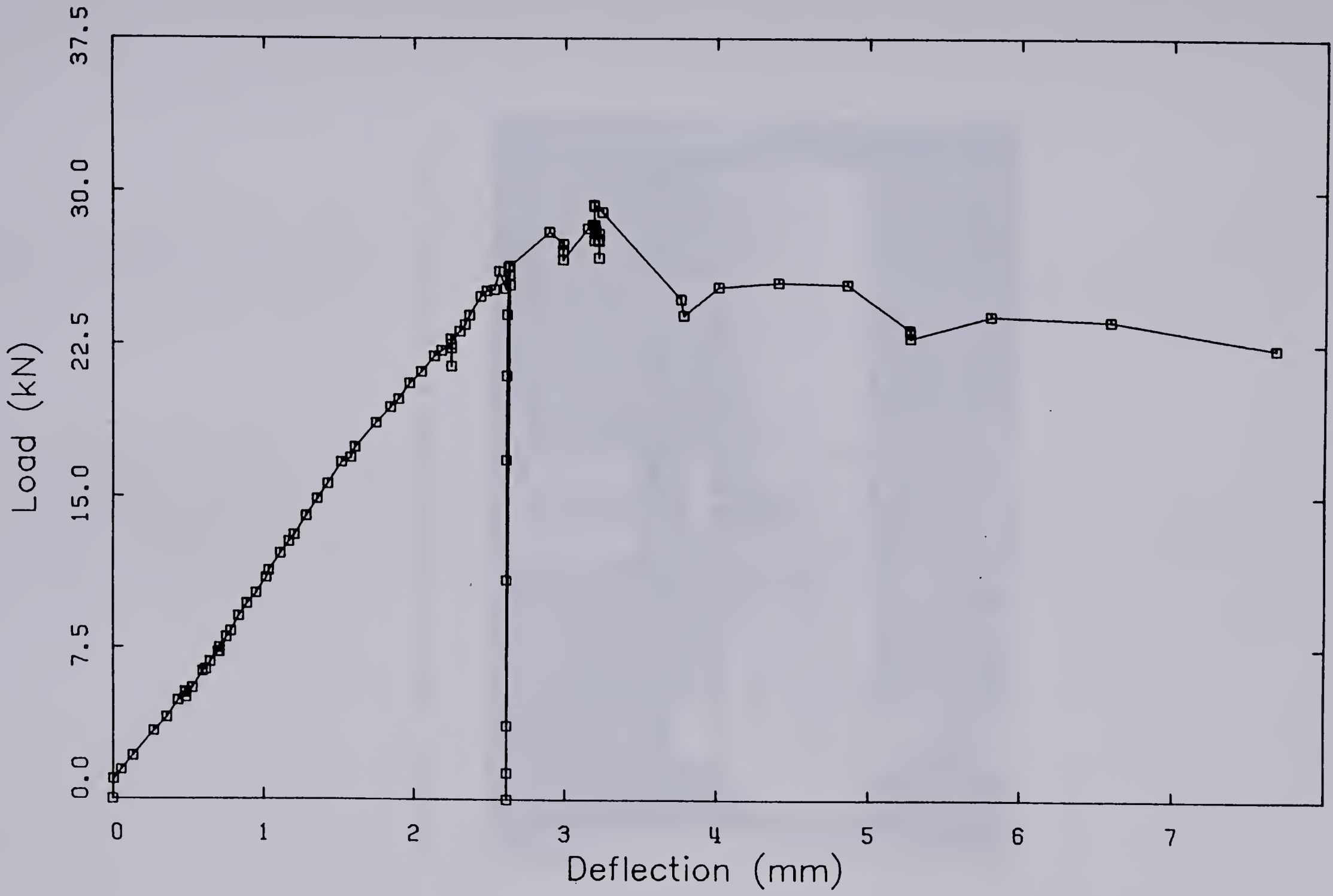

Figure 4.8 Load-Deflection Behaviour of First Shear Specimen

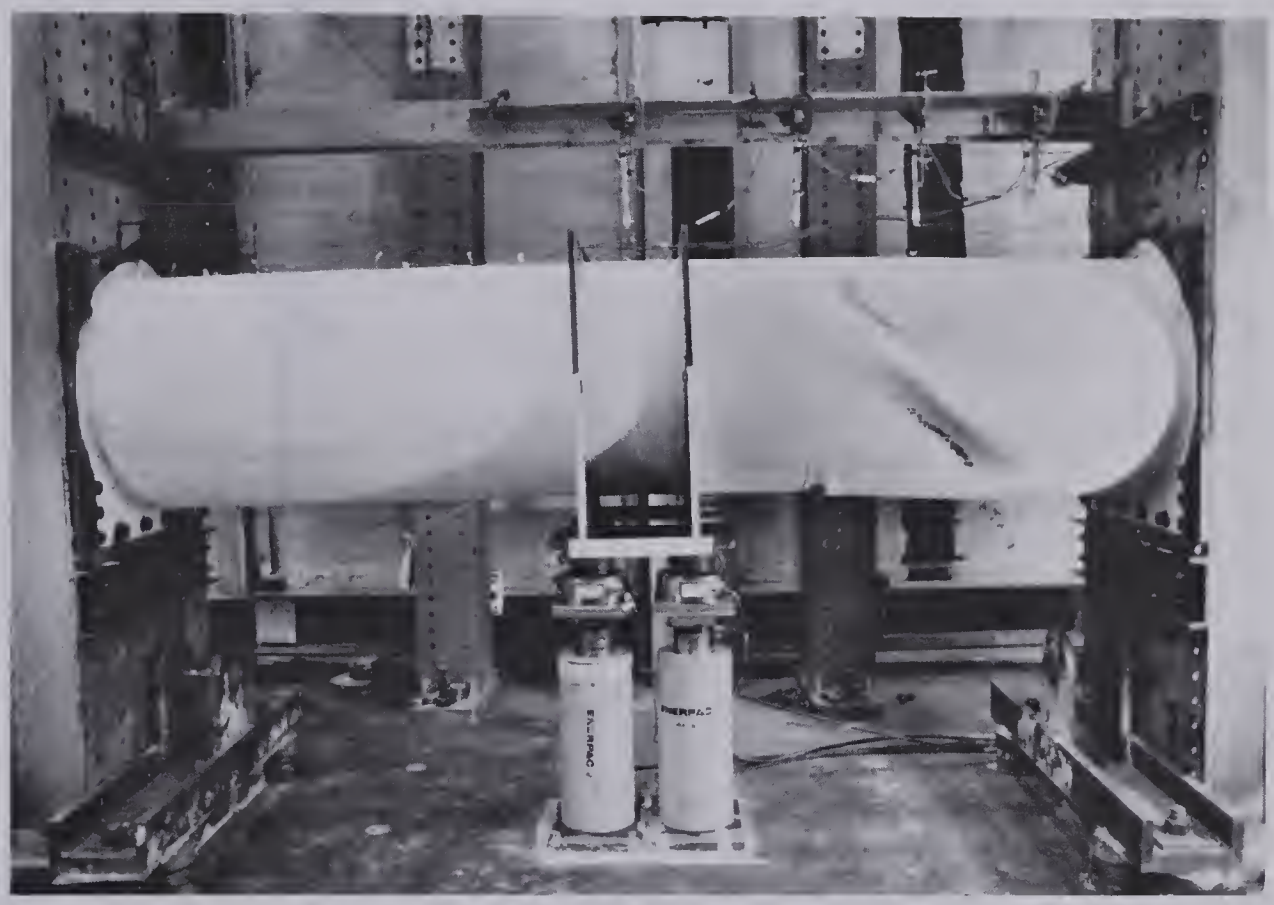

Figure 4.9 Buckled Shape of Second Shear Specimen

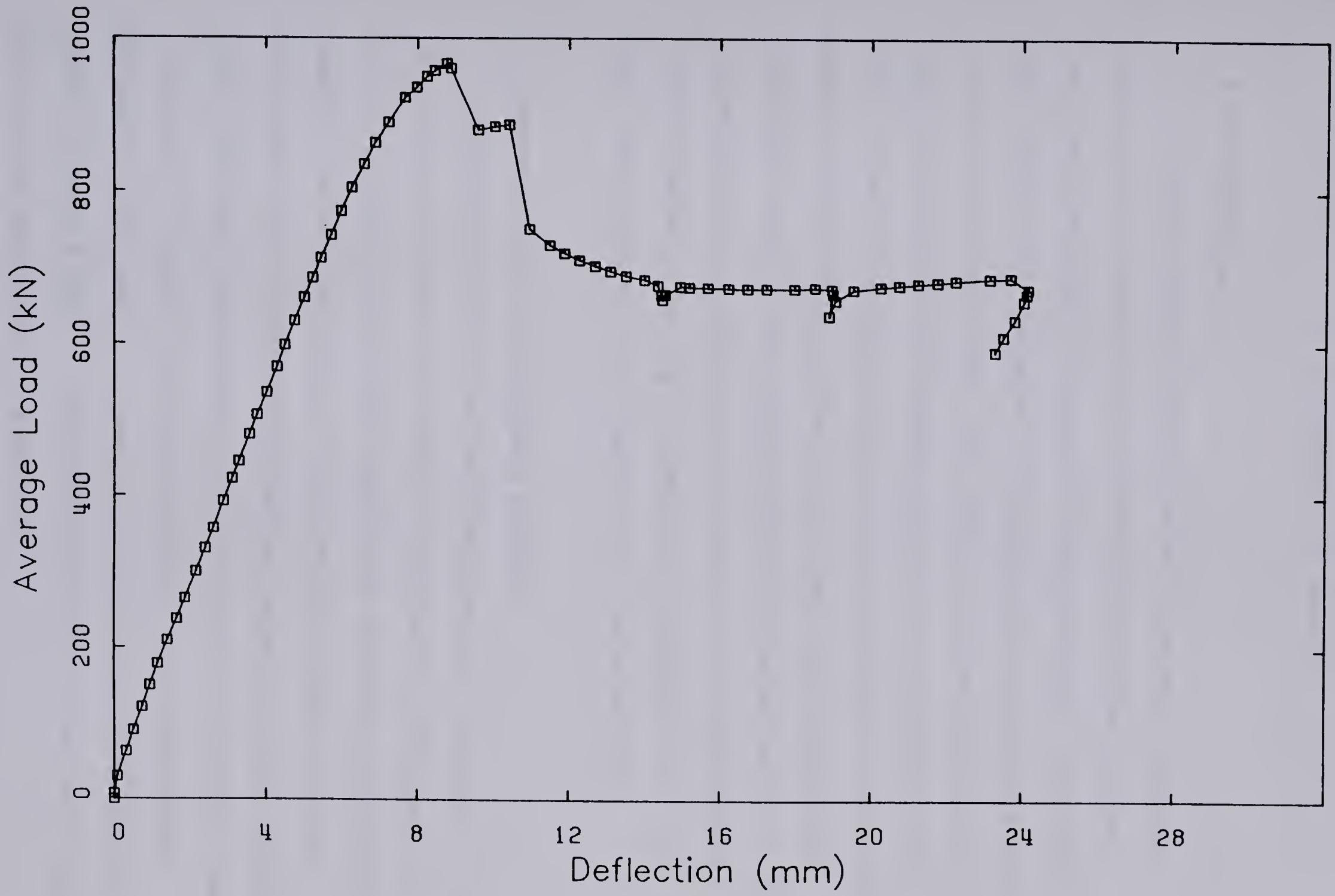

Figure 4.10 Load-Deflection Behaviour of Second Shear Specimen

5. Discussion of Results

5.1 Introduction

In this chapter comparisons made between the test results and corresponding values as determined by the theories presented in Chapter 2 are discussed. The bending test results are compared with predicted strengths and previous experimental work. The results of the bending test on the longitudinally stiffened cylinder are compared first with a prediction for an unstiffened cylinder of otherwise similar shell characteristics and then with predictions using the simplified strength model discussed earlier. Various methods for predicting the behaviour of unstiffened shells loaded primarily in shear are presented, and the shear test results are compared with these methods.

5.2 Behaviour of Unstiffened Cylinder

Figure 5.1 plots the buckling strength obtained in this test along with the test results obtained by Stephens, et al. (1) as well as the semi-empirical strength curve developed by those researchers. The curve is a best-fit curve developed for unstiffened cylinders loaded in axial compression. Although the Stephens, et al. results indicate a small increase in flexural buckling strength over compressive strength, this was not found to be the case with the test result reported herein; the flexural buckling strength was 99% of that predicted by the curve.

Although the number of test results is small, it can be noted that as the parameter $\gamma_s = (E/\sigma_{y_s})^{1/2}(t/R)^{3/2}$ decreases in value, the agreement between the test results and the curve improves. This is at least consistent with what would be expected. The Stephens, et al. equation was developed from work on cylinders under axial compression, which have a uniform strain on the cross section. The flexural tests will have a strain gradient due to the bending stresses, but in general, a cylinder with a lower γ_s will have a higher R/t, causing this strain gradient to approach that of an axially compressed cylinder. For unstiffened fabricated steel tubes with values of γ_s in the range of 0.005 - 0.02, continued use of the curve is warranted for flexure.

5.3 Behaviour of Longitudinally Stiffened Cylinder

As discussed in Section 2.3.1, the geometry and spacing of the stiffeners can be expected to have a large effect on the buckling strength. As a starting point for discussing the flexural strength of the stiffened shell, the theoretical strength of a similar but unstiffened shell as well as a stiffened shell in axial compression are determined. As the semi-empirical equations developed by Stephens, et al. give reasonable results for cylinders tested in flexure, these are used for the shell under consideration. The measured characteristics of the unstiffened shell are

$E = 202\ 900$ MPa, $\sigma_{y_s} = 338$ MPa, $t = 5.0$ mm and $R = 648$ mm,

with a corresponding value of γ_s of 0.0166. Using Eq. 2.4 the value of σ_u/σ_{ys} was calculated to be 0.755, giving a value for σ_u of 255 MPa. Using beam theory, the ultimate moment of this cylinder was calculated to be 841 kN·m. The actual maximum moment achieved in the test was 3068 kN·m, or 3.6 times the predicted buckling load of an unstiffened cylinder of the same dimensions and material properties, while the moment at first yield was observed to be about 1700 kN·m, approximately 2.0 times the predicted buckling load.

If the actual stiffened shell characteristics are used, simple beam theory can be used to calculate the moment at first yield of the stiffeners or shell, whichever governs. In this case the shell yields first, at a moment of 2980 kN·m. The actual moment capacity of the shell (3068 kN·m) was, therefore, only 3% greater than the moment predicted to produce first yield. However, first yield was actually observed at 1700 kN·m, only 57% of first yield according to elastic beam theory.

To establish the strength of a stiffened cylinder with identical material properties and geometry to that tested but loaded under axial compression, two methods are used. These are the Det norske Veritas (DnV) recommendations for offshore structures, 1977 (24), and the method developed by Walker and Sridharan (21), which is discussed in Section 2.3.1.

The DnV (1977) rules state that the buckling resistance of a stringer stiffened cylinder can be calculated using the method given for stiffened plate panels if it is felt that the advantage of curvature will not greatly increase the strength. The rules recognize three types of failure:

1. Plate-induced failure; local buckling of the panels.
2. Stiffener-induced failure; lateral buckling of the stiffeners.
3. Torsional buckling of the stiffeners.

Torsional buckling of the stiffeners can be disregarded if the h/t ratio for the web of the stiffener is less than $1.4\ (E/\sigma_y)^{1/2}$. For the test under consideration, the value of h/t satisfies this condition, as h/t = 13.3, with a limiting value of 27.1.

Because the DnV rules are for design, coefficients to account for uncertainty in load and in material strength are used. In order to compare the DnV rules with the test results obtained herein, the various coefficients used in the equations must be set equal to unity. The calculations for stiffener-induced failure and for plate-induced failure then give, respectively, failure stresses of 164.5 Mpa and 155.1 Mpa. These correspond to elastic failure moments of 1581 and 1491 kN·m for the stiffener and plate, respectively. These results are plotted on the moment versus curvature behaviour diagram in Fig. 5.2. As seen in Fig. 5.2, the moment versus curvature behaviour began to deviate from elastic behaviour at about 1700 kN·m, which is about 14%

greater than the predicted value of 1491 kN·m. It should be realized that the predicted value was calculated for a flat plate, thus neglecting the possible beneficial effect of curvature, and that the theory assumes axial loads, while the test value is that for compression due to bending.

The method of Walker and Sridharan (21) defines two types of cylinder behaviour, broad and narrow. The analysis method used for a narrow-panelled cylinder establishes the load at which first yielding of the stiffener or shell will occur. Broad-panelled theory is used to establish the load at first buckling of the shell. The cylinder classification is dependent on the spacing of the stiffeners. Using Eq. 2.7, the theoretical stiffener spacing, ϕ_{cr}, below which panel behaviour becomes "narrow", must be less than 0.303 radians or 17.4°. The actual stiffener spacing was 19°, which corresponds to 1.09 ϕ_{cr}. If the clear distance between the stiffeners is used, the spacing between stiffeners is 16.8°, which is close to ϕ_{cr} (97%). The cylinder is, therefore, of an intermediate type, between broad and narrow-panelled.

A description of the failure mode of broad and narrow panelled cylinders is given by Walker and Sridharan (21). A broad-panelled cylinder will fail by local buckling of the plate between stiffeners with no overall deflection of the shell-stiffener combination, and with unstable post-buckling behaviour. A narrow-panelled cylinder will fail by overall buckling, with a stable post-buckling behaviour. It was

observed, however, that the specimen's mode of failure included both local and overall buckling, see Section 4.4.2. This behaviour is that of an intermediate cylinder, having both broad and narrow-panelled failure characteristics. The post-buckling behaviour was stable, with the cylinder capable of sustaining additional load. As the buckle pattern was that of an overall type buckling mode, it was thought that the cylinder behaved as a narrow-panelled cylinder.

Accordingly, analysis proceeded using the method given for narrow panels. A computer program was written to handle the iterative computations needed, following recommendations given in Ref. 22. It was necessary to include an estimate of initial imperfections. Based on the findings of Stephens, et al. (1), for flexural specimens, nondimensional amplitudes of initial imperfections (a_o, the ratio of imperfection amplitude to the shell thickness) of 0.25 and 0.75 were used.

Two methods of analysis can be used for narrow-panelled cylinders, depending on whether fixed or pinned ends are assumed. The analytical model predicted that first yield of the column model would occur in the plate at a stress corresponding to a moment of 3090 kN·m for a_o of 0.25, and 2735 kN·m for a_o of 0.75, both for fixed ends. For pinned ends, the values would be 2710 kN·m and 2440 kN·m, respectively. These results are plotted on the moment versus curvature behaviour diagram in Fig. 5.3. The response curve shown in Fig. 5.3 indicates that first yield occurred at a moment of

about 1700 kN·m. This is much lower than any of the predicted values. Furthermore, the first visual observations of yielding were not within the test section but were in the stiffer end regions.

Broad panel theory requires an estimate of the compressive residual stress level present in the panel. In the case under consideration, residual stresses result from two main sources, the fabrication of the cylinder, and the subsequent welding of the stiffeners to the shell. If the residual stress level is assumed to be 30% of the yield stress in the plate, Walker and Sridharan's broad-panelled theory predicts a stress at first buckling which corresponds to a moment of 1750 kN·m, lower than the moment of 2200 kN·m when buckles were first noticed. However, if a residual stress of 20% of the yield value is assumed, the first buckling moment is predicted to be 2080 kN·m, while a 40% value corresponds to a predicted moment of 1430 kN·m. These results are plotted on the moment versus curvature behaviour diagram in Fig. 5.4. Prediction of the moment at first buckling is seen to be quite sensitive to the assumed value of residual stress. A change of 10% in the assumed residual stress level leads to a change in the predicted first buckling moment of approximately 19%.

The method of Walker and Sridharan does not accurately predict the strength of the cylinder under consideration. The narrow-panelled method greatly overestimates the moment at first yield, and the broad-panelled method is

conservative in predicting the moment at first buckling, although this is greatly dependent on the residual stress level assumed.

It is conceivable that broad-panelled behaviour caused buckling of the shell and consequent loss of support for the stiffeners. The stiffeners would then start to move with the shell under the action of a flexural stress gradient, giving the appearance of a narrow-panelled behaviour.

It must be remembered, however, that the methods of Walker and Sridharan are for broad or narrow-panelled cylinders with integral plate stiffeners under axial compression. The cylinder under consideration is a flexurally loaded cylinder of an intermediate type with stiffeners fabricated from HSS material and connected with discrete stitch welds.

In summary, it can be seen that adding the stiffeners greatly increases the strength of a similar but unstiffened shell. The strength of the shell loaded in flexure is 14% in excess of that predicted by the DnV rules (24) for a similarly stiffened flat plate. Finally, it is believed that buckling is precipitated by the shell according to Walker and Sridharan (21).

5.4 Behaviour of Cylinders In Shear

The ultimate strength of fabricated steel cylinders loaded in transverse shear is governed by many factors. These can be divided into three groups, the specimen geometry, the material properties, and the support and loading

conditions. Failure can occur as a result of buckling of the shell, or as a result of stresses exceeding the shear yield value, or, if a tension field forms, because the tension yield stress is exceeded.

As noted in Section 2.4, Batdorf, et al. (30) developed theoretical solutions for curved rectangular panels loaded in shear. Solutions are available for a complete cylinder, for either simply supported or clamped ends. For the first test reported herein (R/t = 251), the critical buckling stress according to Batdorf, et al. is 105 MPa for simply supported edges, and 120 MPa if the edges are considered to be clamped. For the second test (R/t = 75), the theoretical critical stresses are 462 MPa and 500 MPa, respectively.

A shear yield stress for these cylinders can be calculated by multiplying the cross-sectional area by the measured shear yield stress (taken as $\sigma_{y_s}/\sqrt{3}$) and dividing by the shape factor. For thin-walled cylinders, the shape factor is 2.0. The resulting strengths are 78.9 kN for the first test, and 1068 kN for the second. The corresponding shear yield stresses are 174 MPa and 178 MPa, respectively. Comparing these stresses with those predicted by Batdorf, et al., it is apparent that the first shell would reach the shear buckling stress before yielding in shear, while the second should fail in a plastic mode before it reached the critical shear buckling stress.

Comparing actual test results to the shear yield values, the first test reached 37% of yield, while the

second reached 91%. If compared to the shear buckling loads, failure occurred at 62% and 35%, respectively, if simply supported ends are assumed, and 54% and 32% for clamped ends.

Because buckles due to compressive longitudinal stresses were observed in both cases, an attempt can be made to relate the stress which would be necessary to produce compression buckling to the tension field stress. It should then be possible to calculate the total contribution of the tension field to the total shear capacity. The assumed geometry is shown in Fig. 5.5. The following assumptions have been made:

1. The longitudinal stress in the field is equivalent to the stress at which the cylinder would buckle in flexure.
2. The angle of inclination of the field is found using plate girder equations.
3. The stress in the tension field is constant.

The equations used to calculate the flexural buckling stress, and hence the stress in the tension field, are the semi-empirical strength equations developed by Stephens, et al. (1), and presented in this paper as Eq. 2.2 through Eq. 2.5. The equation used for the angle of inclination (ζ) for a tension field, as found in Refs. 35 and 36, assumes the tension field will take the most efficient form, so as to carry the greatest load. This is modified slightly herein, replacing the aspect ratio of the plate girder web (the

ratio of the panel length to the panel height) with the length to diameter ratio of the shear span of the cylinder. The resulting equation is

$$\zeta = \tan^{-1}[(1 + (L/D)^2)^{1/2} - L/D] \qquad (5.1)$$

The angle obtained from Eq. 5.1 was 23.5° for both specimens. The average angle of inclination of the buckles was measured as 24° for the first test, and 38° for the second.

Given this angle, the arc α covered by the tension field will be

$$\alpha = \pi - \beta \qquad (5.2)$$

where

$$\beta = \cos^{-1}(1 - y_2/R) \qquad (5.3a)$$

$$y_2 = L \cdot \tan\zeta \qquad (5.3b)$$

The developed width of the tension field is then $W = \alpha \cdot R$, or

$$W = [\pi - \cos^{-1}(1 - L \cdot \tan\zeta/R)] \qquad (5.4)$$

Calculation of the vertical force component of this tension field can be carried out by dividing the field into narrow strips of width dW, and summing the vertical force components. This summation can be done through integration.

If the stress in the strip is taken to be σ_u, the vertical force component, dF, in each strip will be

$$dF = dW \cdot \sigma_u \cdot t \cdot \sin\zeta \cdot \sin\phi \qquad (5.5)$$

Expressed as a function of the arc

$$dW = R \cdot d\phi \qquad (5.6)$$

Integrating over α, the arc of the tension field, half the total force is determined, since the field will form on both

sides of the cylinder. The total force, V_t, is written as

$$V_t = 2\int_o^a dF \qquad (5.7)$$

Substituting Eqs. 5.5 and 5.6 into Eq. 5.7 and evaluating, the expression for V_t becomes

$$V_t = 2 \cdot R \cdot \sigma_u \cdot t \cdot [1 - \cos\alpha] \cdot \sin\zeta \qquad (5.8)$$

Using Eq. 5.8, the total shear force V_t was calculated to be 21.8 kN for the first test, and 492 kN for the second. These values are 74% and 51%, respectively, of the measured ultimate shear strengths.

It was observed that the difference in behaviour between the two shear specimens was the load versus deflection response. In the first case it was entirely linear whereas the proportional limit was reached prior to buckling in the second case. Therefore, an alternative way of determining the ultimate shear capacity is to examine the maximum state of stress at a point, including residual stresses. During the fabrication process, the cylinder will undergo plastic deformation, leading to residual stresses in the shell. These stresses may lead to premature buckling or yielding of the cylinder. To investigate yielding behaviour, Von Mises' criterion was used (37):

$$(\sigma_1 - \sigma_2)^2 + \sigma_1^2 + \sigma_2^2 + 6\tau^2 = 2\sigma_y^2 \qquad (5.9)$$

where

σ_1 = stress in the circumferential direction

σ_2 = stress in the longitudinal direction

τ = shear stress

When the cylinder was formed from the original flat plate, residual stresses were induced as a result of the rolling process. An estimate of these residual stresses was made and it was found that these reach a maximum of $0.23\sigma_y$ in the circumferential direction, and $0.08\sigma_y$ in the longitudinal direction for the first specimen, and $0.65\sigma_y$ and $0.18\sigma_y$, respectively, for the second specimen. Substituting these values into Eq. 5.9 and determining the shear stress when yielding occurs, the corresponding load was calculated to be 76 kN for the first specimen, and 700 kN for the second. The load calculated for the first specimen is approximately 2.6 times the observed ultimate strength, while the value for the second specimen is close to the observed proportional limit of 750 kN.

These calculations seem to indicate that the tension field theory gives reasonable results for the first specimen (R/t = 251) while the maximum stress calculation gives reasonable results for the second specimen (R/t = 75). In other words, it appears that the first test specimen failed by buckling before shear yielding could occur, while the second test specimen failed primarily by yielding of the shell leading to buckling. The R/t ratio can be used as an indication of the mode of failure of a shell. For a given yield

strength, shells with a low R/t ratio will tend to fail by the maximum effective stress exceeding the yield stress, leading perhaps to inelastic buckling. Those with a high R/t ratio will buckle before yielding occurs. Shells in an intermediate range may fail due to some interaction of yielding and buckling.

In summary, the main parameters that appear to govern the shear strength of large diameter cylinders are the R/t ratio, the yield stress, and the level of residual stress. Obviously, more test data are required over a larger range of R/t before a rational attempt to develop a strength design equation can be be made. A possible form of the relationships might be

$$V_u = K_{t1} \cdot V_t \qquad \text{(high R/t ratio)} \qquad (5.10a)$$

$$V_u = K_{y1} \cdot V_y + K_{t2} \cdot V_t \qquad \text{(intermediate R/t ratio)} \qquad (5.10b)$$

$$V_u = K_{y2} \cdot V_y \qquad \text{(low R/t ratio)} \qquad (5.10c)$$

where V_u is the ultimate shear strength of the cylinder, V_t the tension field strength, V_y the yield strength of the cylinder, and K_{t1}, K_{t2}, K_{y1}, and K_{y2} are functions of R/t, E, ν and σ_y.

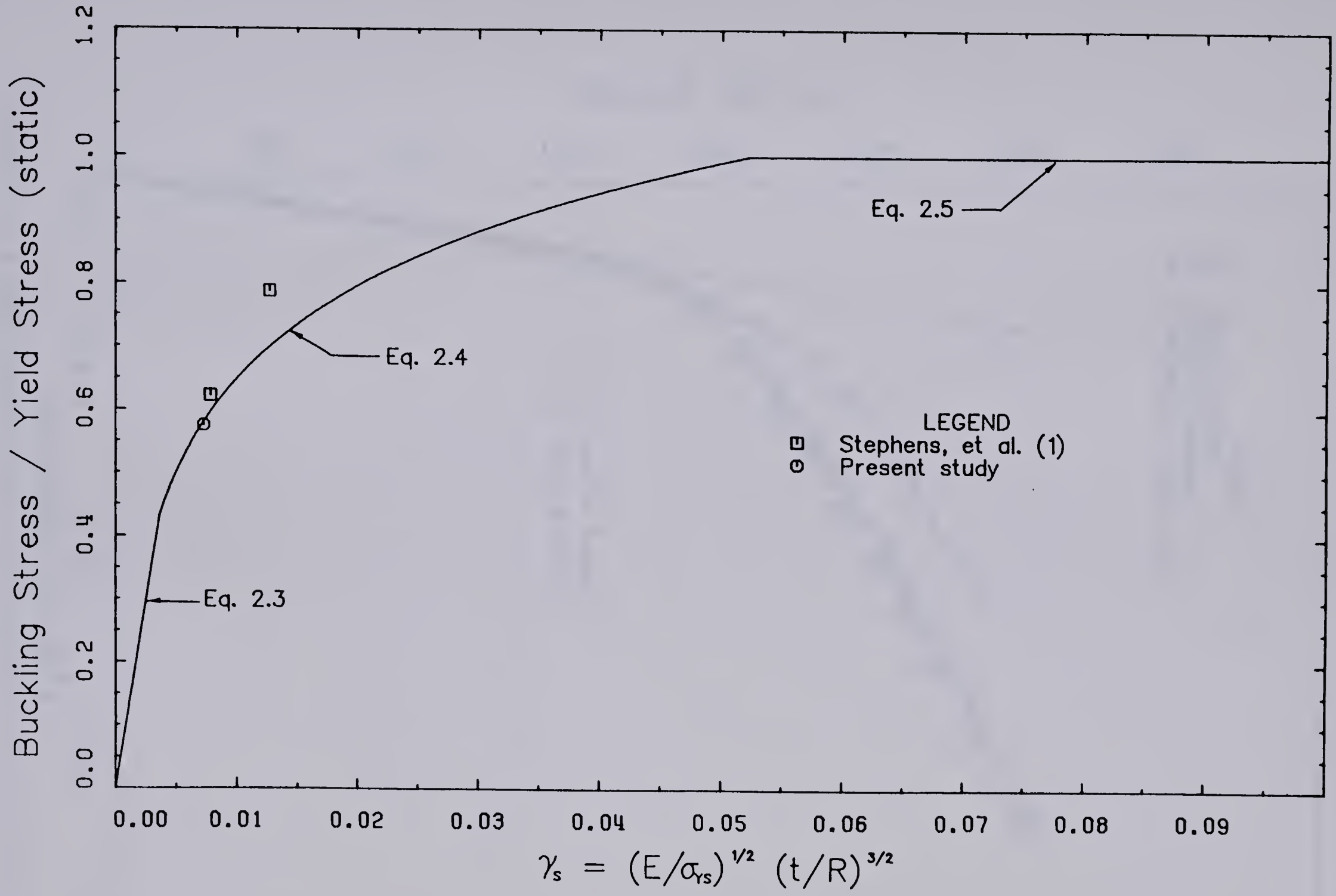

Figure 5.1 Unstiffened Flexural Test Results and Theoretical Strength Curve

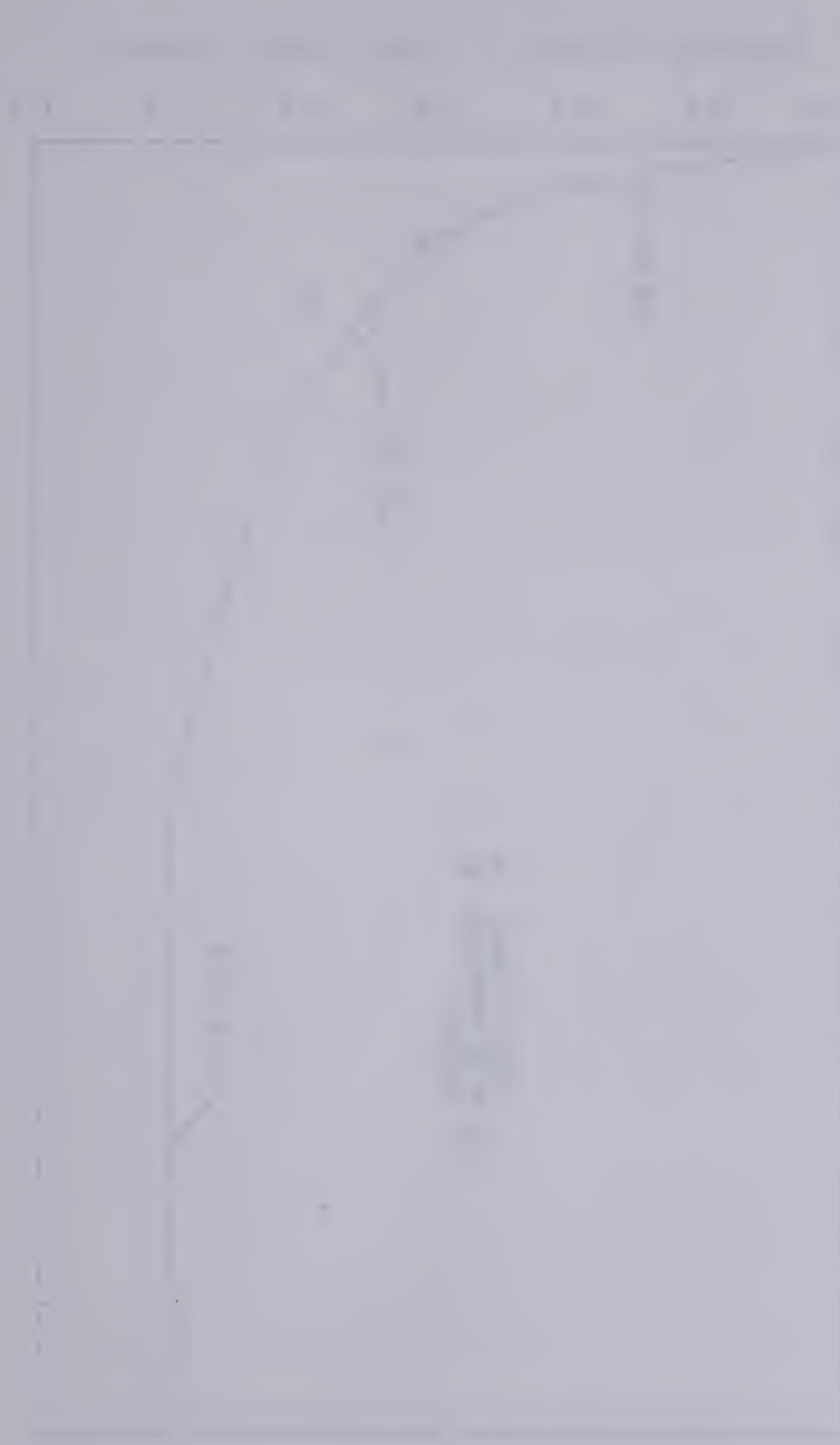

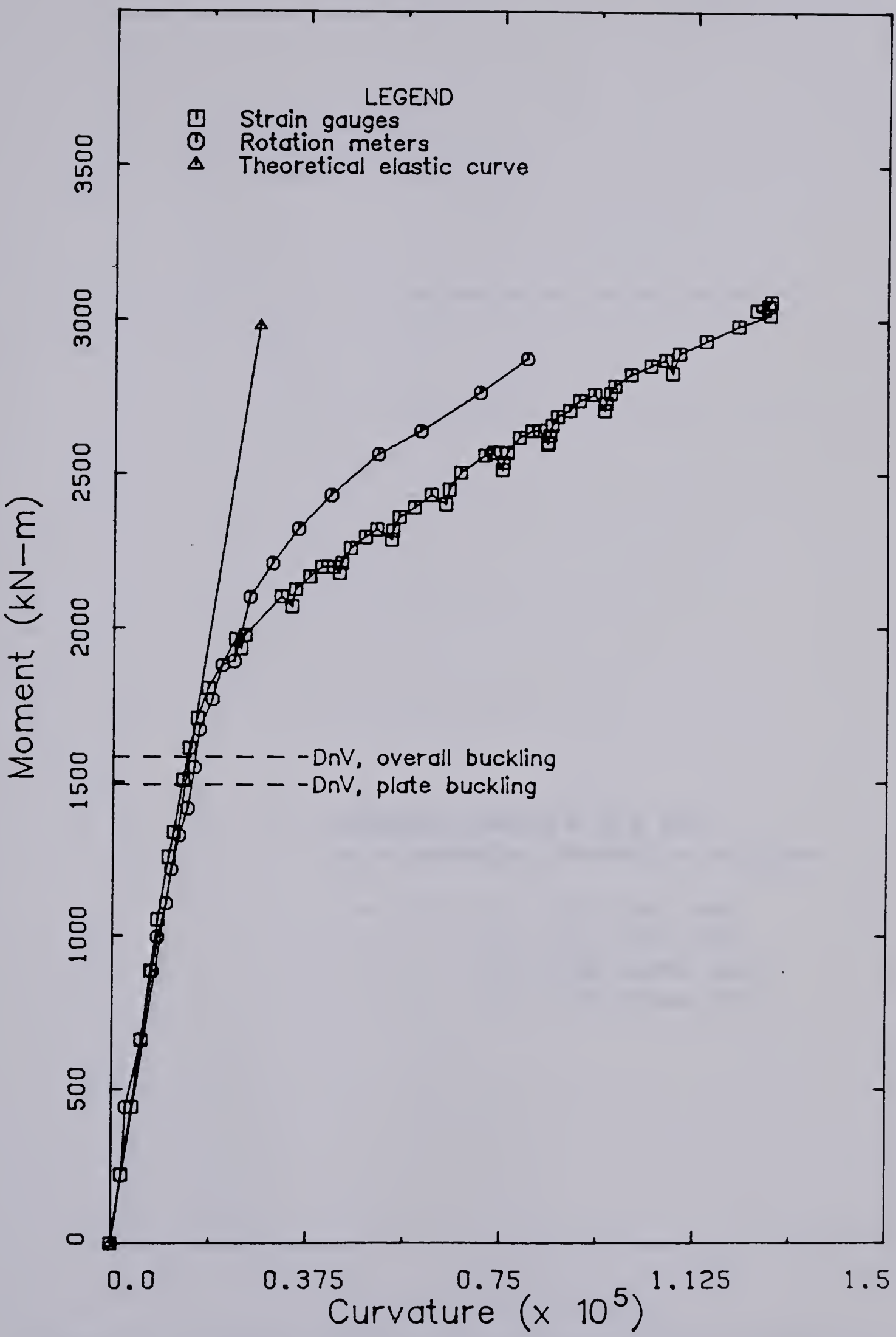

Figure 5.2 DnV Theoretical First Yield for Stiffened Cylinder

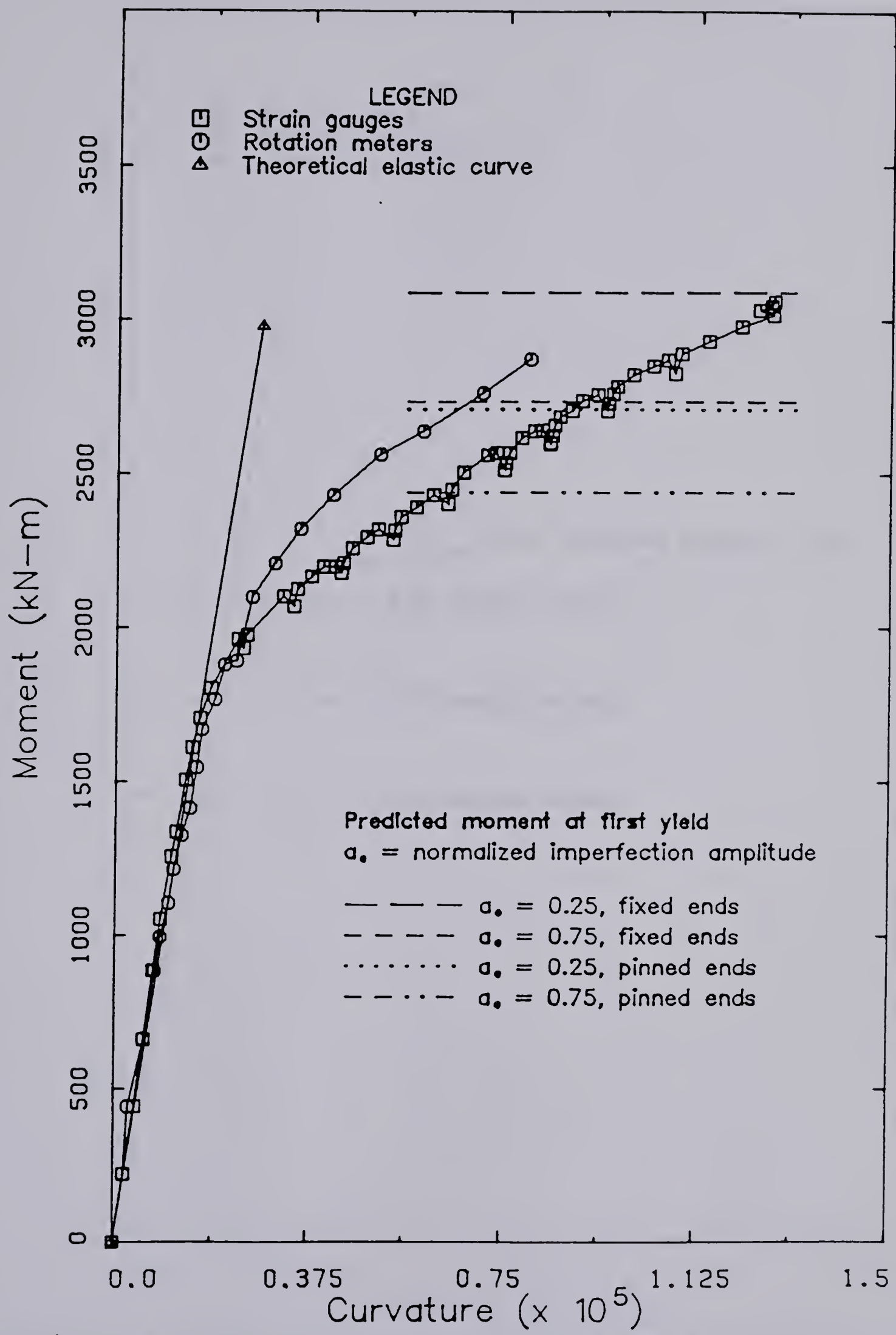

Figure 5.3 Narrow-Panelled Theoretical First Yield for Stiffened Cylinder

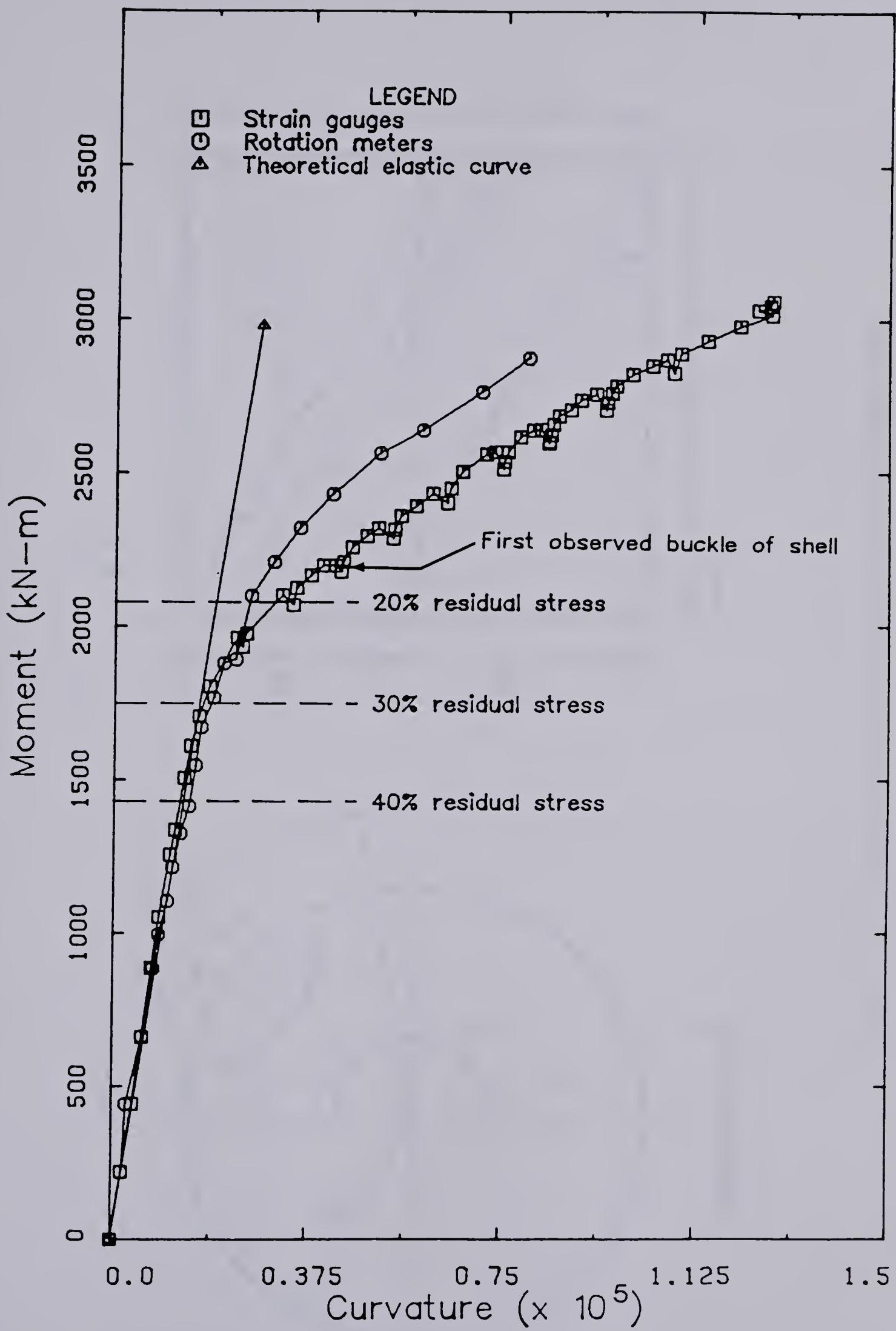

Figure 5.4 Broad-Panelled Theoretical First Buckling for Stiffened Cylinder

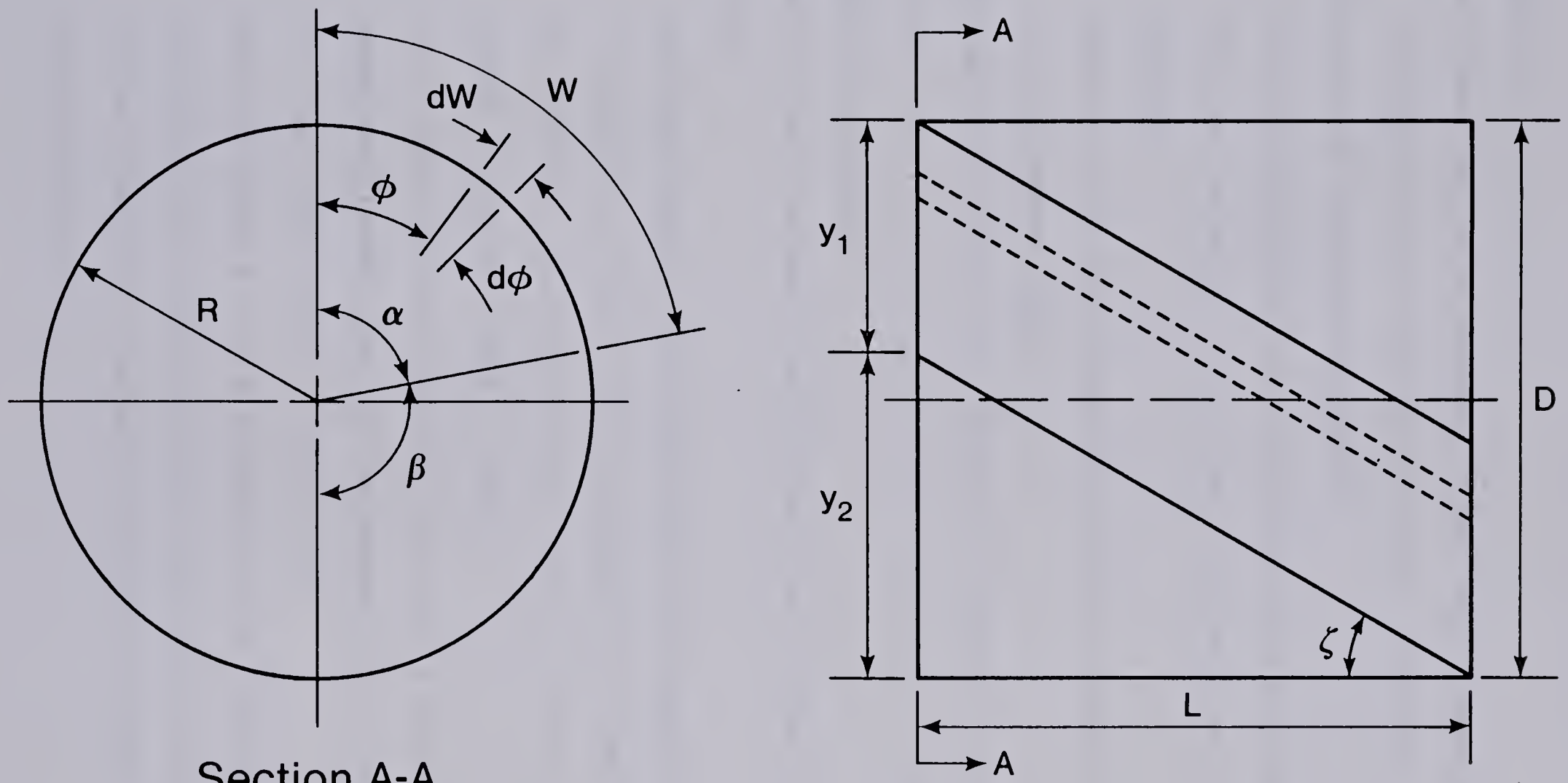

Figure 5.5 Formulation of Tension Field Equations

6. Summary, Conclusions, and Recommendations

6.1 Summary and Conclusions

The investigation discussed herein was undertaken to examine the behaviour of fabricated steel cylinders. The study consists of three main parts:

1. Flexural behaviour of an unstiffened cylinder.
2. Flexural behaviour of a longitudinally stiffened cylinder.
3. Behaviour of unstiffened cylinders loaded primarily in transverse shear.

The experimental phase of the program involved the testing of cylinders manufactured by a steel fabricator using standard shop procedures.

Analysis of the test results has led to the following conclusions:

1. Continued use of the semi-empirical design equation of Stephens, et al. (1) in flexure is justified for unstiffened fabricated steel tubes with values of γ_s in the range of 0.005 - 0.02.
2. Use of longitudinal stiffeners in a flexurally loaded cylinder greatly increases the strength and provides post-buckling stability.
3. The DnV rules for the strength of a longitudinally stiffened flat plate predict the first yield point of the flexurally loaded stiffened cylinder, albeit conservatively.

4. For a stiffened cylinder in the intermediate range, buckling will precipitate as a broad-panelled cylinder, but at a somewhat higher stress.
5. Residual stresses due to the rolling process and the welding of stiffeners have a major role in the buckling strength of broad-panelled longitudinally stiffened cylinders.
6. Residual stresses play a role in premature yielding of a shell in transverse shear. The effect on the buckling behaviour in the elastic range is unknown.
7. The R/t ratio is an important factor in determining the failure mode of a shell in transverse shear. For a given yield strength, shells with a low R/t ratio will tend to fail when the maximum stress exceeds the yield stress, while those with a high R/t value will buckle before yielding occurs.
8. The contribution of the tension field to the shear strength of a cylinder increases as the R/t of the shell increases.
9. There are too few test results at the current time to support the development of a design equation for cylinders loaded in transverse shear.

6.2 Recommendations

1. Further investigation into the buckling strength of unstiffened fabricated steel cylinders loaded in flexure is required. Cylinders with values of γ_s

less than 0.015 should be looked at in both a theoretical and experimental manner.

2. Additional testing of longitudinally stiffened cylinders loaded in flexure is needed in order to investigate the buckling behaviour under varying parameters. These parameters include the spacing, size, and coverage of the stiffeners, the R/t of the shell, and the strengths of the shell and stiffeners.
3. A comprehensive program investigating the strength of fabricated steel cylinders in shear is needed. The investigation should include an experimental study of cylinders of varying R/t ratios loaded in transverse shear. Theoretical work should also be undertaken, including finite element analysis in both the elastic and plastic range.
4. In all cases accurate evaluation of residual stresses due to fabrication and installation is needed.

References

1. Stephens, M. J., Kulak, G. L., and Montgomery, C. J., *Local Buckling of Thin-Walled Tubular Steel Members*, Structural Engineering Report No. 103, Dept. of Civil Engineering, University of Alberta, Feb. 1982.
2. Pinkney, R. B., Stephens, M. J., Murray, D. W., and Kulak, G. L., *Inelastic Buckling of Axially Loaded Cylindrical Shells*, Proceedings, Annual Conference, CSCE, May 27 - 28, 1982, Edmonton, Alberta.
3. Pinkney, R. B., Stephens, M. J., Murray, D. W., and Kulak, G. L., *Use of Measured Imperfections to Predict Buckling of Axially Loaded Cylindrical Shells*, Canadian Journal of Civil Engineering, Vol. 10, No. 4, September, 1983.
4. Timoshenko, S., and Gere, J., Theory of Elastic Stability, McGraw-Hill, New York, N. Y., 1961.
5. Southwell, R. V., *On the General Theory of Elastic Stability*, Phil. Trans. Roy. Soc. Lond., Series A, No. 213, 1914.
6. Flügge, W., *Die Stabilität der Kreiszylinderschale*, Ingen. Arch., Vol. 3, 1932; later reference in: Stresses in Shells, Springer-Verlag, Berlin, 1960.
7. Donnell, L. H., *A New Theory for the Buckling of Thin Cylinders Under Axial Compression and Bending*, ASME Transactions, Vol. 56, 1934.

8. Schilling, C. G., *Buckling Strength of Circular Tubes*, ASCE, J. Structural Division, Vol. 91, No. ST5, Proc. Paper 4520, Oct. 1965.

9. von Kármán, T., and Tsien, H. S., *The Buckling of Thin Cylindrical Shells Under Axial Compression*, J. Aeron. Sci., Vol. 8, No. 8, 1941.

10. Koiter, W. T., *Buckling and Post-Buckling Behaviour of a Cylindrical Panel Under Axial Compression*, Report S 476, National Luchtvaartlaboratorium, Amsterdam, Reports and Transactions, 1956.

11. Arbocz, J., and Babcock, C. D., *Prediction of Buckling Loads Based on Experimentally Measured Initial Imperfections*, Buckling of Structures, edited by B. Budiansky, Springer-Verlag, New York, N. Y., 1976.

12. Arbocz, J., *The Effect of Initial Imperfections on Shell Stability*, Thin-Shell Structures, edited by Y. C. Fung and E. E. Sechler, Prentice-Hall, Englewood Cliffs, N. J., 1974.

13. Babcock, C. D., *Experiments in Shell Buckling*, Thin-Shell Structures, edited by Y. C. Fung and E. E. Sechler, Prentice-Hall, Englewood Cliffs, N. J., 1974.

14. Seide, P., and Weingarten, V. I., *On the Buckling of Circular Cylindrical Shells Under Pure Bending*, Transactions of the ASME, Vol. 28, No. 1, March 1961, Series E.

15. Brazier, L. G., *On the Flexure of Thin Cylindrical Shells and Other 'Thin' Sections*, Proc. Royal Society, London, Series A, Vol. 116, 1927.

16. Seide, P., Weingarten, V. I., and Morgan, E. J., *Elastic Stability of Thin-shell Structures*, Space Technology Labs Report STL/TR-60-000-19425, Dec. 1960.

17. Weingarten, V. I., Morgan, E. J., and Seide, P., *Elastic Stability of Thin-Walled Cylindrical and Conical Shells Under Axial Compression*, AIAA J., Vol. 3, No. 3, March 1965.

18. Walker, A. C., and Sridharan, S., *Buckling of Compressed, Longitudinally Stiffened Cylindrical Shells*, Behaviour of Off-Shore Structures 1979, Vol. 2, paper 72.

19. Baruch, M., and Singer, J., *Effect of Eccentricity of Stiffeners on the General Instability of Stiffened Cylindrical Shells Under Hydrostatic Pressure*, J. Mech. Eng. Science, Vol. 5, No. 1, March 1963.

20. Singer, J., Baruch, M., and Harari, O., *On the Stability of Eccentrically Stiffened Cylindrical Shells Under Axial Compression*, Int. J. of Solids and Structures, 1967, Vol. 3.

21. Walker, A. C., and Sridharan, S., *Analysis of the Behaviour of Axially Compressed Stringer-Stiffened Cylindrical Shells*, Proceedings of the Institution of Civil Engineers, Part 2, June, 1980, Vol. 69.

22. Sridharan, S., and Walker, A. C., *Experimental Investigation of the Buckling Behaviour of Stiffened Cylindrical Shells*, Great Britain Department of Energy Report OT-R7835, 1980.

23. Dowling, P. J., *Research in Great Britain on the Stability of Circular Tubes*, 1982 Structual Stability Research Council Annual Technical Session, New Orleans, 1982.

24. Det norske Veritas, *Rules for the Design Construction and Inspection of Offshore Structures*, Appendix C, Steel Structures, 1977 (Rev. 1982)

25. Valsgard, S., and Foss, G., *Buckling Research in Det norske Veritas*, Buckling of Shells In Offshore Structures Edited by J. E. Harding, P. J. Dowling, and N. Agelidis, Granada, London, 1980.

26. Kurobane, Y., Atsuta, T., and Toma, S., *Research in Japan of the Stability of Circular Tubes*, 1982 Structual Stability Research Council Annual Technical Session, New Orleans, 1982.

27. Miller, C. D., and Grove, R. B., *Current Research Related to Buckling of Shells for Offshore Structures*, 15th Annual Offshore Technology Conference, Houston, Texas, May 1983.

28. Fujita, T., Nakata, Y., Sawayanagi, M., and Matsumoto, Y., *Buckling Strength of Stiffened Cylindrical Shells*, Journal of the Society of Naval Architects of Japan, No. 135, June 1974, in Japanese; later reference in: *Research in Japan of the Stability of Circular Tubes*, 1982 Structual Stability Research Council Annual Technical Session, New Orleans, 1982.

29. Batdorf, S. B., Schildcrout, M., and Stein, M., *Critical Stress of Long Plates With Transverse Curvature*, NACA TN-1346, 1947.

30. Batdorf, S. B., Stein, M., and Schildcrout, M., *Critical Stress of Curved Rectangular Panels*, NACA TN-1348, 1947.

31. Wilson, W. M., and Olson, E. D., *Tests of Cylindrical Shells*, U. of Illinois Engineering Experimental Station Bulletin Series, No. 331, 1941.

32. Basler, K., *Strength of Plate Girders in Shear*, Journal of the Structural Division, ASCE, Vol. 87, No. ST7, Oct. 1961.

33. Structural Stability Research Council, Guide to Stability Design Criteria for Metal Structures, 3rd edition, edited by B. G. Johnston, John Wiley and Sons, New York, N. Y., 1976.

34. Canadian Standards Association, *Structural Quality Steels*, CSA Standard G40.21M, 1978.

35. Salmon, C. G. and Johnson, J. E., Steel Structures - Design and Behavior, Second Edition, Harper and Row, 1980.

36. Adams, P. F., Krentz, H. A., and Kulak, G. L., Limit States Design in Structural Steel, Second Edition, Canadian Institute of Steel Construction, 1979.

37. Ugural, A. C., and Fenster, S. K., Advanced Strength and Applied Elasticity, Elsevier North Holland, 1978.